

THESIS FOR THE DEGREE OF DOCTOR OF PHILOSOPHY IN THERMO AND
FLUID DYNAMICS

On the Analysis of Energy Efficient Aircraft Engines

OSKAR THULIN

Department of Mechanics and Maritime Sciences
Division of Fluid Dynamics
CHALMERS UNIVERSITY OF TECHNOLOGY
Göteborg, Sweden 2017

On the Analysis of Energy Efficient Aircraft Engines
OSKAR THULIN
ISBN 978-91-7597-635-8

© OSKAR THULIN, 2017

Doktorsavhandlingar vid Chalmers tekniska högskola
Ny serie nr. 4316
ISSN 0346-718X

Department of Mechanics and Maritime Sciences
Division of Fluid Dynamics
Chalmers University of Technology
SE-412 96 Göteborg
Sweden
Telephone: +46 (0)31-772 1000

Chalmers Reproservice
Göteborg, Sweden 2017

On the Analysis of Energy Efficient Aircraft Engines
Thesis for the degree of Doctor of Philosophy in Thermo and Fluid Dynamics
OSKAR THULIN
Department of Mechanics and Maritime Sciences
Division of Fluid Dynamics
Chalmers University of Technology

ABSTRACT

Aero engine performance analysis is highly multidimensional using various measures of component performance such as turbomachinery and mechanical efficiencies, and pressure loss coefficients. Using conventional performance analysis, relying on only the laws of thermodynamics, it is possible to understand how the performance parameters affect the component performance, but it is difficult to directly compare the magnitude of various loss sources. A comprehensive framework has been detailed to analyze aero engine loss sources in one common currency. As the common currency yields a measure of the lost work potential in every component, it is used to relate the component performance to the system performance. The theory includes a more detailed layout of all the terms that apply to a propulsion unit than presented before. The framework is here adopted to real gases to be used in state of the art performance codes. Additionally, the framework is further developed to enable detailed studies of two radical intercooling concepts that either rejects the core heat in the outer nacelle surfaces or uses the core heat for powering of a secondary cycle. The theory is also extended upon by presenting the *installed rational efficiency*, a true measure of the propulsion subsystem performance, including the installation effects of the propulsion subsystem as it adds weight and drag that needs to be compensated for in the performance assessment.

Keywords: Aero engine, Aircraft engine, Exergy analysis, Installed propulsion, Performance modelling, Turbofan, Ultra high bypass ratio, Variable area fan nozzle, Translating cowl, Multiple pivoting flaps, Engine weight estimate

“If we all worked on the assumption that what is accepted as true is really true, there would be little hope of advance.”

- Orville Wright

ACKNOWLEDGEMENTS

I would, first and foremost, like to express my sincere appreciation to my main supervisor, Professor Tomas Grönstedt at Chalmers University of Technology, for all the support throughout this work. Thank you for making me want to strive further every day. I also owe my deepest gratitude to my co-supervisor Ph.D. Jean-Michel Rogero at Airbus S.A.S for interest in my research project. Without Tomas’s and Jean-Michel’s extensive knowledge, passion for aviation and for being such nice people to work with, I would not have developed this much nor would it have been this joyful. I also would like to recognize Ph.D. Anthony Roux, Ph.D. Alexandre Neophytou, Ph.D. Anders Lundblad, Ph.D. Olivier Petit, Ph.D. Xin Zhao, and Ph.D. Carlos Xisto for their extensive help and positive collaboration.

A big *thank you* goes out to all the past and present colleagues in the Turbomachinery & Aeroacoustics research group and at the Fluid Dynamics division. I consider it an honor to work with you, and you make the time spent at Chalmers so much more worthwhile.

Finally, I would also like to express my gratitude to Airbus S.A.S. for funding this thesis. Moreover, I also would like to thank the European Commission (E-BREAK program - Seventh Framework Program under the Grant Agreement No. 314366) for funding the variable area fan nozzle research.

NOMENCLATURE

A	Area [m^2]
B	Arbitrary conserved extensive property
C	Velocity with respect to the atmosphere at rest [m/s]
D	Drag force [N]
E	Energy [J]
E_x	Exergy [J]
\dot{E}_x	Exergy rate [J/s]
F	Force [N]
\vec{F}	Vector force [N]
HHV	Higher heating value [J/kg]
L	Lift force [N]
L/D	Lift over drag force coefficient [–]
LHV	Lower heating value [J/kg]
\dot{I}	Irreversibility rate [J/s]
\dot{I}^*	Normalized irreversibility rate [–]
M	Molar mass [kg/mol]
P	Power out of the control volume [J/s]
Q	Heat transfer into the control volume [J]
\dot{Q}	Heat transfer rate into the control volume [J/s]
R	Specific gas constant [$J/(kgK)$]
S	Entropy [J/K]
SFC	Specific fuel consumption [$mg/(Ns)$]
T	Temperature [K]
U	Velocity of propulsion unit relative to the atmosphere at rest [m/s]
V	Velocity relative to the reference frame of the propulsion unit [m/s], Volume [m^3]
W	Work [J]
a	Acceleration [m/s^2], Number of carbon atoms in a fuel molecule
b	Number of hydrogen atoms in a fuel molecule
c	Number of sulfur atoms in a fuel molecule
\vec{c}	Vector velocity with respect to the atmosphere at rest [m/s]
c_p	Specific heat capacity [$J/(kgK)$]
d	Number of oxygen atoms in a fuel molecule
e	Specific energy [J/kg], Number of nitrogen atoms in a fuel molecule
\vec{f}	Force vector field [N/kg] i.e. [m/s^2]
g	Specific Gibbs free energy [J/kg], Gravitational constant [m/s^2]
h	Specific enthalpy [J/kg]
m	Mass [kg]
\dot{m}	Mass flow rate [kg/s]
\hat{n}	Unit normal vector [–]
p	Pressure [N/m^2]
\dot{q}	Body heating vector field [$J/(kgs)$]

s	Specific entropy [$J/(kgK)$]
t	Time [s]
\vec{u}	Vector velocity of propulsion unit relative to the atmosphere at rest [m/s]
\vec{v}	General vector velocity [m/s], Vector velocity relative to the reference frame of the aircraft [m/s]
x	Mole fractions [-]
y	Mass fractions [-]
Δ	Difference
Δ_f°	Thermodynamical property of formation at standard state conditions
$\dot{\Pi}$	Entropy production rate [$J/(sK)$]
Ψ	Rational efficiency [-]
α	Angle of attack [$^\circ$]
β	Mass fractions in fuel [-], Arbitrary conserved intensive property
γ	Path angle [$^\circ$], Liquid activity coefficient [-]
δ	Deviation angle between the aircraft's direction and the engine's direction [$^\circ$]
ε	Specific exergy [J/kg]
ζ	Mass fraction of environmental species per unit resource species [-]
η	Energy efficiency [-]
θ	Attitude [$^\circ$]
λ	Mass fraction of combustion products per unit burned fuel [-]
ν	General stoichiometric coefficient
ϕ	Angle between flight trajectory and thrust vector [$^\circ$]
$\vec{\phi}_q$	Heat flux [J/m^2s]
ρ	Density [kg/m^3]
$\vec{\tau}$	Shear stress vector [N/m^2]

Subscripts/Superscripts

CS	Control surface
CS open	Open control surface
CS closed	Closed control surface
CV	Control volume
D	Drag
L	Lift
S	Shaft
T	Thrust
W	Weight
cs	Closed system
g	Gross thrust
i	Index of summation in components / mass constituents
in	Into control volume
j	Index of summation over components
n	Upper bound of summation
md	Momentum drag
net	Net thrust

out	Out of control volume
pot.	Potential
prop. syst.	Aircraft propulsion system
prop. unit	Aircraft propulsion unit
rad.	Radiation
rel.	Relative
ss	Standard state
surf.	Surface
syst.	System level
th.	Thermomechanical
t	Total properties relative to the propulsion unit
∞	Ambient condition
0	Total properties relative to the atmosphere at rest

THESIS

This thesis consists of an extended summary and the following appended papers:

- Paper A** O. Thulin, J.M. Rogero and T. Grönstedt, 2015, “A Mission Assessment of Aero Engine Losses, *International Society for Airbreathing Engines*,“ ISABE-2015-20121, Arizona, USA
- Paper B** T. Grönstedt, M. Irannezhad, L. Xu, O. Thulin, A. Lundbladh, “*First and Second Law Analysis of Future Aircraft Engines*,” *Journal of Engineering For Gas Turbines and Power*, vol. 136, no. 3, 2014.
- Paper C** X. Zhao, O. Thulin and T Grönstedt, “*First and Second Law Analysis of Intercooled Turbofan Engine*,” *Journal of Engineering For Gas Turbines and Power*, vol. 138, no. 2, 2015.
- Paper D** O. Thulin, O. Petit, C. Xisto, X. Zhao and T. Grönstedt, “*First and Second Law Analysis of Radical Intercooling Concepts*,” *Journal of Engineering For Gas Turbines and Power*, 2017.
- Paper E** O. Thulin, A. Lundbladh, and T. Grönstedt, “*Variable Area Fan Nozzle Weight and Performance Modeling*,” To be submitted for publication in a scientific journal, 2017.

CONTENTS

Abstract	i
Acknowledgements	iii
Nomenclature	v
Thesis	ix
Contents	xi
I Extended Summary	1
1 Introduction	1
1.1 Purpose	4
2 Exergy and Propulsion	5
2.1 Exergy Applied to Propulsion	5
2.2 Exergy Fundamentals	7
2.2.1 First Law of Thermodynamics	8
2.2.2 Second Law of Thermodynamics	11
2.2.3 Combining the First and Second Law of Thermodynamics	13
2.3 Fuel Exergy	26
2.3.1 Fuel Exergy Combustion Modeling	30
2.3.2 Possibility of Omitting the Chemical Mixing Exergy to Ambient Air	32
2.4 Application of Exergy to Non-standard Propulsion Components	33
2.4.1 Exergy Analysis of Heat Exchangers	33
2.4.2 Exergy Analysis in Closed systems	35
2.4.3 Exergy Analysis of Exhaust Gases	36
3 Exergy and Aircraft Performance	39
3.1 Relation between Exergy and Conventional Performance	39
3.2 Installation Effects on Exergy	40
3.2.1 Propulsion System Exergy Assessment	45
3.2.2 Installed Rational Efficiency	47
3.2.3 Mission Assessment	48
3.3 CFD-based Exergy Analysis for Aircraft-Integrated Propulsion Units	49
4 Variable Area Fan Nozzles	51
4.1 Translation of Rearmost Part of the Nacelle	51
4.2 Multiple Pivoting Flaps	52

5	An Exergy Assessment of Modern Aircraft Engines and the Way Forward	53
5.1	State of the Art Aircraft Engines	53
5.1.1	Ejected Heat	55
5.1.2	Combustion	55
5.1.3	Non-propulsive Kinetic Power	56
5.2	The Way Forward	57
5.2.1	Ejected Heat	58
5.2.2	Combustion	59
5.2.3	Non-propulsive Kinetic Power	61
6	Summary of Papers	63
6.1	Paper A: A Mission Assessment of Aero Engine Losses	63
6.2	Paper B: First and Second Law Analysis of Future Aircraft Engines	63
6.3	Paper C: First and Second Law Analysis of Intercooled Turbofan Engine	64
6.4	Paper D: First and Second Law Analysis of Radical Intercooling Concepts	64
6.5	Paper E: Variable Area Fan Nozzle Weight and Performance Modeling	64
7	Summary of Contribution	67
II	Appended Papers A–E	73

Part I

Extended Summary

1 Introduction

Achieving more efficient aircraft and propulsion systems is of paramount importance in the aerospace industry. Propulsion system development, selection, and integration pose a complex challenge as it constitutes a highly multidimensional and tightly coupled system. Performance studies based on the first law of thermodynamics illustrate how the parameters, such as turbomachinery efficiencies, mechanical efficiencies, and pressure loss coefficients, affect the component performance but does not give any information how the component behavior relates to the overall performance. The conventional way to assess potential improvements of propulsion units through parametric studies on a baseline model does not allow for a way to make the losses comprehensible, only to study the effect of an incremental change. The exergy methodology allows for analysis that assess the component contribution to the overall losses in a unified framework, and thus, also makes it possible to relate the different component losses to each other.

Using the exergy methodology allows analysis of the engine performance in one common currency, that fully takes advantage of the possibilities in the first and second law of thermodynamics. Exergy calculations relate the thermodynamical properties of a fluid stream to an equilibrium state to determine the work potential at each station in the engine. The further away the thermodynamical properties are from the equilibrium state, the larger the work potential is. Tracking the loss of work potential in each component throughout the cycle clearly indicates where the irreversibilities occur. This will lead to a more illustrative way of presenting the losses, and thus, enable a better understanding of how the component losses relate to the system performance. Moreover, the developed framework detailed in this thesis can be used to address the loss sources in an aero engine more systematically and to explore innovative propulsion unit architectures in search for lower fuel consumption and consequently reduced emissions.

Horlock and Clark pioneered the field of exergy analysis by applying it to a turbojet as early as 1975 [1]. Their original work was derived from extending the work of Evans [2]. In 1995, Brilliant extended the analysis for a turbofan engine [3] which was studied at the cruise point. Roth and Mavris published a series of papers assessing the performance of a Northrop F-5E “Tiger II” lightweight fighter plane, powered by two J85-GE-21 turbojets, including a full mission study from 2000 [4]. Rosen provided a mission analysis of a commercial turbofan in 2009. However, the assumed engine performance and flight conditions were far from a typical airline operation which led to that the analysis fails to provide a good understanding of the typical distribution of the loss sources.

Grönstedt et al. used exergy analysis in the cruise point to evaluate different future commercial engine concepts including a turbofan reference corresponding to a technology

level assumed to be available the year 2050, an intercooled and recuperated engine, a pulse detonation combustion engine and an open rotor engine [5]. Zhao et al. continued the exploration of exergy analysis by applying it to better understand the benefits of intercooling in turbofan aero engines [6]. Thulin et al. published a mission study of a commercial turbofan in 2015 that provided analysis of the main mission points that constitutes a commercial mission [7]. The studied engine was more specifically of a direct-drive two-shaft type set up to represent a technology level maturity corresponding to the year 2020. The engine architecture was chosen due to its dominating market share in modern aviation. The analysis did not only include the engine assessment in terms of the thermodynamic cycle but rather the full impact of the propulsion system including the weight and drag that inherently needs to be compensated for by engine. The exergy framework was later extended to include a detailed analysis of two radical intercooling concepts [8]. The first use the already available nacelle surface to reject core heat and contribute to an overall drag reduction. The second uses the rejected heat to power a secondary Rankine cycle and produce useful power to the aircraft-engine system.

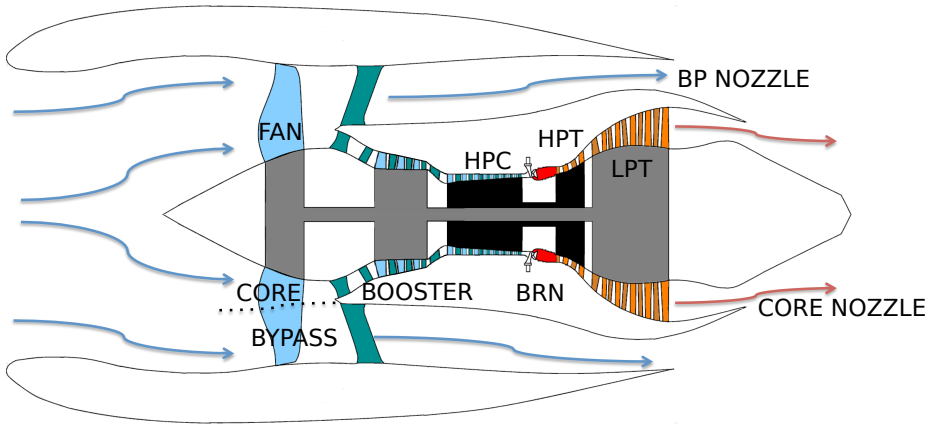


Figure 1.1: Schematic of a direct-drive two-shaft type turbofan with the main components denoted.

As illustrated in Fig.1.1 the engine takes in cold air and adds work to it in the ducted fan (FAN). The air is then divided into a bypass flow and a core flow. This split is the fundamental difference between the turbofan and a turbojet, as the latter instead lets all mass flow go through a single passage that works similar to the turbofan core. The bypass flow continues via the bypass duct and out through the bypass nozzle where it is accelerated to create a propulsive force that propels the aircraft forward. The fan cannot run without any power supply, and this is where the core flow comes in. The air that is directed through the core flow is then pressurized in two compressors. For a two-shaft turbofan, as illustrated in the picture, these are called booster and high-pressure compressor (HPC). The fan and the booster are powered by the same shaft while the high-pressure compressor is powered by a second shaft. Fuel is injected into the compressed air in the combustor (BRN) where the air and fuel mixture also is ignited. The combustion process

increases the energy of the gas. Parts of the energy in the flow is extracted downstream in the two turbines, the high-pressure turbine, and the low-pressure turbine, to power the compressors and fan on the respective shaft. The gas mix then exits the core nozzle to add to the propulsive force that propels the aircraft.

To give an indication of the value an exergy analysis can offer for the analysis of the engine irreversibilities a total system assessment is illustrated in Fig.1.2 and Fig.1.3. About thirty percent of the total work potential in the fuel is useful for the aircraft. Another four percent is lost due to the installation effects of the engine in terms of the added weight and drag that needs to be compensated for. About two-thirds is lost as irreversibilities in the propulsion unit. These irreversibilities are divided into groups corresponding to the different sources in the engine irreversibility breakdown. The direct feedback of how the losses relate to the system performance is made very transparent by adding exergy analysis next to the conventional performance analysis.

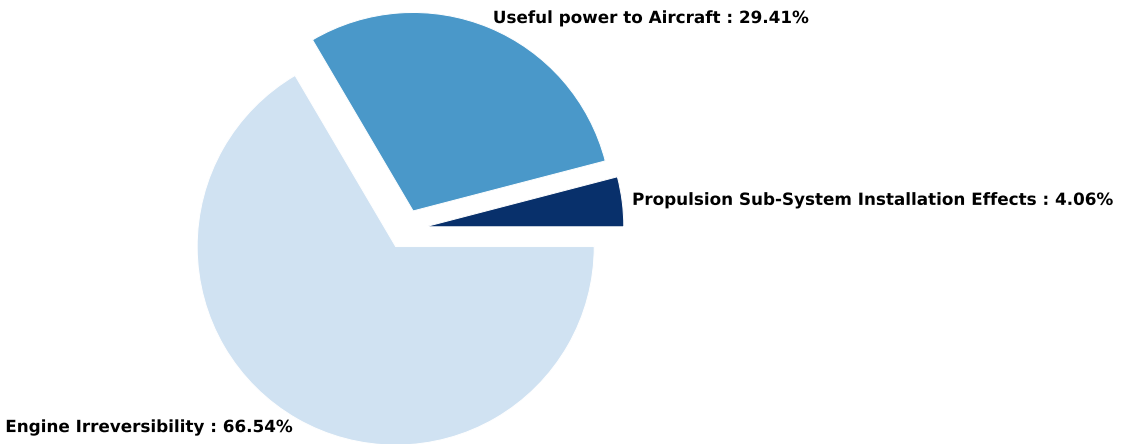


Figure 1.2: A simplified short mission total exergy breakdown for a modern turbofan (Thulin et al. 2015 [7]).

The major irreversibilities of the turbofan can be seen to be the thermal energy in hot exhaust gases that is leaving the engine. Keeping this term low relates to a high thermal efficiency, which is dependent on high pressure ratios, and consequently, in the general case high temperatures ratios. The irreversibility in the combustor makes up a significant contribution as combustion inherently is a process under which substantial amounts of entropy is generated. Furthermore, the non-propulsive kinetic energy also stands for a notable part. The propulsive efficiency relates the useful thrust power and the non-propulsive kinetic irreversibility by effectively being calculated by the thrust power divided by the sum of both terms. By lowering the specific thrust, i.e. the velocity increase

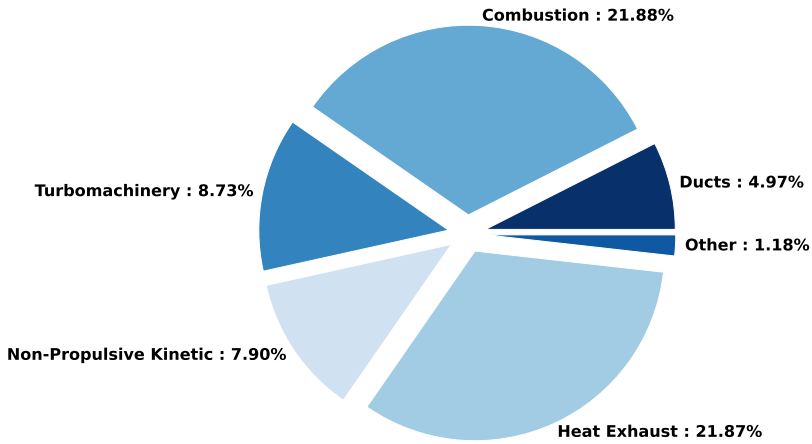


Figure 1.3: A simplified short mission engine irreversibility breakdown of a modern turbofan (Thulin et al. 2015 [7]). When the irreversibility percentages are summed up they correspond to the engine irreversibilities divided by the provided fuel exergy as illustrated in Fig.1.3.

of the mass flow, a higher propulsive efficiency can be achieved. To maintain the thrust requirement, a larger mass flow through the engine is now needed. The turbofan engine is able to achieve a high thermal efficiency by its high pressure ratio in the core and at the same time a high propulsive efficiency by "bypassing" vast amounts of flow at a low degree of velocity increase in the bypass section.

By development of higher power-density core cycles and by increasing the ratio between the bypass and the core flow, the bypass ratio, BPR, it is possible to increase the thermal and the propulsive efficiencies further. Such turbofans that feature lower specific thrust magnitudes than today also experience more varying operating conditions throughout the flight envelope, and therefore, poses a considerable matching problem in obtaining acceptable performance and at the same time reasonable safety margin towards critical operation in any of the operation points. To allow for the more varying operation different types of variability functionalities have been suggested. For this reason the author has also studied the performance and installation of a variable area fan nozzle [9].

1.1 Purpose

The purpose of this work has been to quantify the losses in aircraft propulsion units in a more systematic and illustrative way. By using the developed framework better understanding of the component losses can be enabled. Knowing how the component losses relates to the system performance can then be utilized in the search for more efficient engine configurations.

2 Exergy and Propulsion

This chapter details exergy applied to propulsion which is a central concept in this thesis. It starts by describing the fundamental control volume exergy equations and continues by deriving and presenting the terms used in the exergy equations. The assessment also includes how radical propulsion unit components can be handled and presents how component irreversibilities can be broken up further detail than commonly presented in context of propulsion unit performance calculations.

2.1 Exergy Applied to Propulsion

The most significant energy fluxes in an aero component are thrust, mechanical work, kinetic energy, thermomechanical energy, chemical energy, and heat. Therefore the exergy analysis presented herein, based on the work of Horlock and Clark [1], includes all these aforementioned fluxes. In Horlock and Clark's analysis, the formulation is derived with the perfect gas assumption. However, the present formulation includes real gas behavior allowing it to be used in state of the art aero-engine performance codes with semi-perfect gas tables.

The maximum work that can be obtained for an aero engine system is given by Eq. 2.1 and is illustrated in Fig. 2.1. This formulation is a result of combining the first and second law of thermodynamics.

$$\left(\sum_i \dot{m}_i \varepsilon_i \right)_{\text{in}} \geq P_S + P_T - \sum_i \int \frac{T - T_\infty}{T} d\dot{Q}_i + \left(\sum_i \dot{m}_i \varepsilon_i \right)_{\text{out}} \quad (2.1)$$

where \dot{m}_i = mass flow rate through open control volume boundary of index i

ε_i = specific exergy of mass flow through open control volume boundary of index i , detailed in Eq. 2.26 & Eq. 2.48

P_T = thrust power extracted from the control volume, detailed in Eq. 2.33-2.35

P_S = shaft power extracted from the control volume

\dot{Q}_i = heat transfer rate through the control volume boundary of index i and directed inwards, detailed in Eq. 2.37, 2.39-2.42

T = temperature at heat transfer

The maximum work is obtained in the reversible limit at which equality holds [10]. The equation corresponds to the exergy balance of the incoming and outgoing exergy fluxes and is a measure of the irreversibility of the system.

The irreversibility rate, also called the exergy destruction rate, \dot{I} , is formed as a difference when bookkeeping the exergy crossing the boundaries of a control volume:

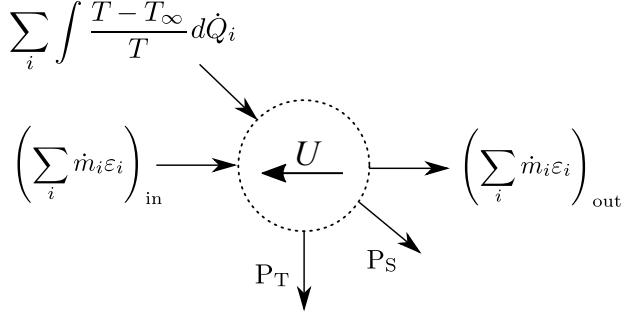


Figure 2.1: Exergy applied to the reference frame of the engine

$$\dot{I} = \left(\sum_i \dot{m}_i \varepsilon_i \right)_{\text{in}} - \left(\sum_i \dot{m}_i \varepsilon_i \right)_{\text{out}} - P_S - P_T + \sum_i \int \frac{T - T_\infty}{T} d\dot{Q}_i. \quad (2.2)$$

Relating the component irreversibilities to the total input of exergy, $\dot{E}_{x,\text{total input}}$, gives the ratio of irreversibility for each component, then

$$\dot{I}^* = \frac{\dot{I}}{\dot{E}_{x,\text{total input}}}. \quad (2.3)$$

Summing up all the irreversibility contributions forms the total irreversibility

$$\dot{I}^*_{\text{system}} = \frac{\sum_j \dot{I}_j}{\dot{E}_{x,\text{total input}}}. \quad (2.4)$$

The rational efficiency expresses the useful work of a control volume in relation to the incoming exergy flux. The useful power generated by the aero engine is the thrust provided to the aircraft as well as the other useful power terms, such as the cabin bleed and power that the propulsion system potentially supplies to the cabin. Cabin bleed and power are not commonly included in the rational efficiency term. However, since they provide useful work for the aircraft they should be included in the useful work term, and therefore we define

$$\Psi_{\text{system}} = \frac{P_{T\text{prop. unit}} + P_{\text{other useful}}}{\dot{E}_{x,\text{total input}}}, \quad (2.5)$$

where $P_{\text{other useful}}$ can be but is not limited to

$$P_{\text{other useful}} = [(\dot{m}\varepsilon)_{\text{bleed}} + P_s]_{\text{cabin}}.$$

It is noteworthy that the rational efficiency is equal to one minus the total irreversibility ratio, i.e. $\Psi_{\text{system}} = 1 - \dot{I}^*_{\text{system}}$, as any output that is not seen as useful for a system must be a loss of useful potential.

Note that when the reference environment is set to the ambient conditions, the total magnitude of exergy that enters into the system is equal to the exergy of the injected energy source. For airbreathing jet engine, this equals the exergy within the injected fuel, i.e.

$$\dot{E}_{x,\text{total input}} = \dot{m}_{\text{fuel}}\varepsilon_{\text{fuel}}. \quad (2.6)$$

However, if another means of energy source would be used to power the propulsion unit, this would instead be included in this term. For example, a systematic analysis of a battery-powered aircraft could be enabled by including the change in exergy of the battery as the total exergy input.

2.2 Exergy Fundamentals

By using the gas enthalpy, it is possible to quantify the energy difference between the fluid stream at an arbitrary station in an engine to when the fluid stream is in equilibrium with its surroundings. Part of this energy will, however, be inaccessible even if the fluid stream is taken to equilibrium in an ideal process. The equilibrium temperature multiplied by the entropy difference between the fluid stream and equilibrium state quantifies the energy that is inaccessible. Combining the total energy and the inaccessible energy yields the work potential, i.e. the exergy,

$$\text{Exergy} = \text{Work potential} = \text{Total energy} - \text{Inaccessible energy}. \quad (2.7)$$

The ambient conditions outside the engine stretches far enough for the equilibrium state not to change from the initial surroundings. Thus, the equilibrium in propulsion unit exergy analysis is taken as that of the ambient temperature, pressure, and chemical composition.

A more elaborate form of the irreversibility rate presented in Eq. 2.2 is now derived from its contributing formulations, and its terms are detailed to be used for aero engine calculations. To assess how much of the work potential is lost in an arbitrary propulsion unit component, a combination of the first and second law of thermodynamics can be used. It is possible to use Reynold's transport theorem [11] to construct an open system control volume formulation for a conserved thermodynamic property, it reads

$$\underbrace{\frac{dB}{dt}}_{\text{Input}} \Big|_{\text{system}} = \underbrace{\frac{d}{dt} \left(\int_{\text{CV}} \rho\beta dV \right)}_{\text{Change (per time)}} + \underbrace{\int_{\text{CS}} \rho\beta (\vec{v}_{\text{rel}} \cdot \hat{n}) dA}_{\text{Flow out minus in}}. \quad (2.8)$$

In the theorem B is any extensive property that is conserved, and β is the intensive equivalent. The vector velocity \vec{v} is the absolute velocity in perspective of the reference frame and \vec{v}_{rel} quantifies the relative velocity to the control surface.

2.2.1 First Law of Thermodynamics

The law of conservation of energy states that energy can neither be created nor destroyed; rather, it can only be transformed from one form to another. Within thermodynamics, this is known as the first law of thermodynamics and states that the difference in work and heat will balance the difference of energy within the differential. Mathematically, using Clasius' sign convention for heat and work, this is expressed as:

$$\delta Q - \delta W = dE \quad (2.9)$$

An open system per time unit formulation is sought for. Therefore, the differential is rewritten on a per time unit basis to the following equation:

$$\delta \dot{Q} - \delta P = \frac{dE}{dt} \quad (2.10)$$

Using Reynold's transport theorem to obtain an open system formulation for the extensive property E yields heat and work, both per unit time, over the system boundary as the input terms on the left-hand side of the equation. On the right-hand side, the first term represents the change of energy held within the system and the second quantifies the energy associated with every mass particle passing the system boundary. The intensive quantity, β , equals the total energy per mass denoted with e_0 . The equation becomes

$$\dot{Q} - P = \frac{d}{dt} \left(\int_{CV} \rho e_0 dV \right) + \int_{CS} \rho e_0 (\vec{v}_{rel.} \cdot \hat{n}) dA, \quad (2.11)$$

where e_0 corresponds to the internal energy, kinetic energy, and a term collecting other contributions, namely $u + \frac{\|\vec{v}\|^2}{2} + e_{other}$. Other contributions could cover chemical reactions, nuclear reactions and electrostatic or magnetic field effects.

Work per unit time, i.e. power, can originate from various sources and is typically calculated as the scalar product of the force vector multiplied with the absolute velocity vector. The different forces that act on the system are body forces such as gravity, forces on the boundaries such as shear and pressure, and reaction forces within the system boundaries that can be lumped in specific terms such as shaft work. Inserting these terms into the Reynold's transport theorem for energy conservation yields

$$\begin{aligned} \dot{Q} - \overbrace{P_S}^{\text{Shaft}} + \overbrace{\int_{CV} \rho \vec{f} \cdot \vec{v} dV}^{\text{Body forces}} + \overbrace{\int_{CS} \vec{\tau} \cdot \vec{v} dA}^{\text{Shear stress}} - \overbrace{\int_{CS} p (\vec{v} \cdot \hat{n}) dA}^{\text{Pressure}} = \\ \frac{d}{dt} \left(\int_{CV} \rho \left(u + \frac{\|\vec{v}\|^2}{2} + e_{other} \right) dV \right) + \int_{CS} \rho \left(u + \frac{\|\vec{v}\|^2}{2} + e_{other} \right) (\vec{v}_{rel.} \cdot \hat{n}) dA. \end{aligned} \quad (2.12)$$

The specific exergy formulation found later in Sec. 2.2.3 use enthalpy to quantify the thermomechanical energy as enthalpy also directly includes the energy to make room for the system by replacing its surroundings. Thus, both the control volume and the control

surface terms are here adapted accordingly. To allow for the change the identity is used by which the specific internal energy relates to the enthalpy, i.e. $u + \frac{p}{\rho} = h$. The use of enthalpy herein can be seen more evident for the control surface integral than the control volume integral which can be seen below.

Starting with the control volume an enthalpy term forms when adding the $\frac{p}{\rho}$ inside the volume integral. To balance the terms a negative $\frac{p}{\rho}$ is also placed within the volume integral. This additional term is the additional pressure-volume work that must be made to accommodate a change within the system with respect to time.

It can be noted that the pressure power term and the control surface mass flow term share resembling features. It is possible to alternate the expression to get enthalpy which includes the part of the pressure power term originating from the relative velocity. This part of the pressure work on the boundary equals the net energy to make room for the flux by displacing its surroundings. Since the control surface mass flow term will only have fluxes through the open control volume surfaces it is also possible to alter the integral interval to only open surfaces. Moreover, the left-hand side pressure power term can include both on closed and open boundaries. For this reason, the integral is split into two terms where one is affected by the pressure that does work on the boundary.

By considering the particular case of a propulsion unit, it is possible to neglect several terms based on their respective magnitude. Gravity is the only body force acting on the mass flow in the system, and it is weak in comparison to the other terms. Moreover, for the general case of gas in an aero engine, the e_{other} term can be left out. Any specific energy from a chemical reaction can be included when necessary in the internal energy/enthalpy term, for the case of the combustor, this is included as the heat of combustion. The resulting equation taking the enthalpy-internal energy alternation and the neglected terms into account becomes

$$\begin{aligned} \dot{Q}_{\text{in}} - P_S + \int_{\text{CS}} \vec{\tau} \cdot \vec{v} dA - \int_{\text{CS}} \vec{v} \cdot \hat{n} dA - \int_{\text{CS}_{\text{open}}} p(\vec{v} - \vec{v}_{\text{rel.}}) \cdot \hat{n} dA - \int_{\text{CS}_{\text{closed}}} p\vec{v} \cdot \hat{n} dA = \\ \frac{d}{dt} \left(\int_{\text{CV}} \rho \left[h - \frac{p}{\rho} + \frac{\|\vec{v}\|^2}{2} \right] dV \right) + \int_{\text{CS}_{\text{open}}} \rho \left(h + \frac{\|\vec{v}\|^2}{2} \right) (\vec{v}_{\text{rel.}} \cdot \hat{n}) dA. \end{aligned} \quad (2.13)$$

The relative velocity relates to the absolute velocity by the surface velocity, i.e. $\vec{v}_{\text{rel.}} = \vec{v} - \vec{v}_{\text{surf.}}$. Using a reference frame that is moving with the control volume and assuming that the open control volume surfaces are fixed relative the control volume lead to cancellation of the left-hand side pressure power term. Secondly, it also enables writing the velocity relative to the reference frame where the velocity relative the control surface previously has been stated.

As a consequence of the choice of a reference system moving with the control volume the viscosity integral and the pressure integral are both zero at all stationary closed surfaces

due to non-slip conditions. In system control volume formulations of turbomachinery components, the boundaries are generally put enclosing the whole component, and not on the surface of the turbomachinery. Therefore, the work is lumped into one term, e.g. the P_S term, which was previously introduced. The viscosity is handled using a turbomachinery efficiency. Ducts and similar components do not, in general, have any moving control surfaces and therefore the viscosity work is zero for such components.

One type of component that may exist within a propulsion unit system where the pressure integral for closed surfaces is different from zero is a piston engine. However, piston engines are not integral components in commercial aircraft propulsion units of today. Even if the opposite were the case, the piston engine's cyclic behavior would likely be modeled in a propulsion unit system performance analysis by using time-averaged properties and a shaft power term.

At open surfaces, the viscous terms can still be different from zero, especially if there are control volume formulations with open boundaries parallel to the flow and with very different fluid velocities. However, for such an event the mixing would likely be modeled using a mixing efficiency and pressure loss coefficient within one control volume formulation. For flow normal to a boundary the power integral will be small in comparison to the other power terms.

By the consideration of components that may include pressure work on the closed boundaries as well as how viscous effects are included into system analysis it can be concluded that these terms can be omitted. The updated formulation reads:

$$\dot{Q} - P_S = \frac{d}{dt} \left(\int_{CV} \rho \left[h - \frac{p}{\rho} + \frac{\|\vec{v}\|^2}{2} \right] dV \right) + \int_{CS_{open}} \rho \left(h + \frac{\|\vec{v}\|^2}{2} \right) (\vec{v} \cdot \hat{n}) dA. \quad (2.14)$$

If a reference level is imposed for enthalpy and set to the ambient conditions, the energy difference to the equilibrium state is quantified. This form is useful to assess exergy which is quantified as the difference in accessible energy between the true conditions and the equilibrium conditions. By addition and subtraction of the same integral with h_∞ on the right-hand side of the equation it is possible to include a reference level into the surface integral term. The added integral can be shown to represent the mass flow over the boundary multiplied with h_∞ . Due to mass conservation, the net difference between the mass flow over the boundary must be equal to the negative change per time unit of mass within the system. Therefore, the additional h_∞ -integral can be included into the volume integral as a reference which leads to the updated formulation:

$$\begin{aligned} \dot{Q} - P_S = & \frac{d}{dt} \left(\int_{CV} \rho \left[h - h_\infty - \frac{p}{\rho} + \frac{\|\vec{v}\|^2}{2} \right] dV \right) \\ & + \int_{CS_{open}} \rho \left(h - h_\infty + \frac{\|\vec{v}\|^2}{2} \right) (\vec{v} \cdot \hat{n}) dA. \end{aligned} \quad (2.15)$$

The velocity magnitude in the right-hand integrals is preferred to be expressed using the velocity relative to the atmosphere at rest, \vec{c} , as the term then quantifies the kinetic power compared to the equilibrium state with an atmosphere at rest for the mass particles passing the control volume boundary. Rearranging the control surface equation from above so that the velocity relative atmosphere at rest is used rather than the control volume relative velocity, \vec{v} , give the addition of a thrust power term, P_T . The use of the velocity relative atmosphere at rest in the volume integral is enabled by collecting the change of velocity and the pressure-volume terms that are associated with the system changing per time unit into a new term $P_{\text{sys. change}}$. The new steady state energy equation becomes:

$$\begin{aligned} \dot{Q} - P_S - P_T - P_{\text{sys. change}} &= \frac{d}{dt} \left(\int_{CV} \rho \left[h - h_\infty + \frac{\|\vec{c}\|^2}{2} \right] dV \right) \\ &+ \int_{CS_{\text{open}}} \rho \left(h - h_\infty + \frac{\|\vec{c}\|^2}{2} \right) (\vec{v} \cdot \hat{n}) dA, \end{aligned} \quad (2.16)$$

where the thrust power term equals

$$P_T = \int_{CS_{\text{open}}} \rho \left(\frac{\|\vec{v}\|^2}{2} - \frac{\|\vec{c}\|^2}{2} \right) (\vec{v} \cdot \hat{n}) dA \quad (2.17)$$

and the power associated with the change per time unit corresponds to

$$P_{\text{sys. change}} = - \frac{d}{dt} \left(\int_{CV} \rho \left[\frac{\|\vec{c}\|^2}{2} - \frac{\|\vec{v}\|^2}{2} + \frac{p}{\rho} \right] dV \right). \quad (2.18)$$

Choosing the velocity relative to the atmosphere at rest rather than the ground has two advantages; the magnitude of the velocity relative atmosphere at rest can be used to obtain the whole difference towards the equilibrium state, whereas using the ground speed would require the inclusion of a wind speed kinetic energy term. Secondly, it will be coherent with the thrust power calculations used in engine performance codes where the wind is not included in the flight speed, which is vital since work in Newtonian physics is dependent on the reference frame.

2.2.2 Second Law of Thermodynamics

All processes always take place in accordance with the first law of thermodynamics mentioned above. In addition, a natural process also has a preferred direction of action; this leads to a part of the energy being inaccessible. According to Clausius [12]:

Heat can never pass from a colder to a warmer body without some other change, connected therewith, occurring at the same time.

This statement is also known as Clausius statement and is one of the formulations of the second law of thermodynamics. In fact, there are multiple statements for this law that all lead to equivalent results despite being expressed in different ways. Sadi Carnot should also be mentioned among those who have contributed to the formulation as he was the first to outline the law in 1824 [13] by stating that the efficiency of a reversible cycle between two temperature reservoirs is only dependent on the temperature magnitudes of the reservoirs. Kelvin-Planck also contributed with a statement that reads [14]:

It is impossible for any device that operates on a cycle to receive heat from a single reservoir and produce a net amount of work.

That is, 100% thermal efficiency is not obtainable. All these formulations clearly put a maximum limit to the obtainable work.

A key concept relating to the second law of thermodynamics is the thermodynamics property entropy, which was discovered and named by Clausius in 1865 [15]. It can be seen as a measure of how far a system is taken towards complete equilibrium. When a system has reached equilibrium the entropy within the system has maximized, and at this point work output is no longer obtainable by any process taking place within the system. Entropy is designated S , and by using Clausius inequality the following differential is obtained

$$\frac{\delta Q}{T} \geq dS \quad (2.19)$$

The difference between the right-hand side and the left-hand side is the entropy generated in an irreversible process. By introducing a term called entropy production that corresponds to the difference and is denoted Π , the inequality can be closed. Therefore it follows:

$$\frac{\delta Q}{T} + \delta \Pi = dS \quad (2.20)$$

An open system formulation per time unit is sought for. Thus, the equation from above is rewritten to be stated on a per time basis.

$$\frac{\delta \dot{Q}}{T} + \delta \dot{\Pi} = \frac{dS}{dt} \quad (2.21)$$

Using Reynold's transport theorem for the extensive property entropy, S , leads to the following open system per time unit formulation of entropy

$$\dot{\Pi} + \int \frac{d\dot{Q}}{T} = \frac{d}{dt} \left(\int_{CV} \rho s dV \right) + \int_{CS} \rho s (\vec{v}_{rel.} \cdot \hat{n}) dA. \quad (2.22)$$

It shall be noted that Reynold's transport theorem is only valid for a conserved property, which entropy is not. However, by the addition of the entropy production rate term the equation is conserved and usage of Reynold's transport theorem becomes possible.

The entropy reference level is set to the ambient conditions as this later enables quantifying the inaccessible energy difference to the equilibrium state. Moreover, it is possible to relate the irreversibility rate mentioned in Eq. 2.2 solely with the change in entropy. To do this the heat transfer rate over temperature integral is first moved to the other side of the equal sign to have the entropy production rate standalone. The updated equation becomes:

$$\dot{\Pi} = \frac{d}{dt} \left(\int_{CV} \rho [s - s_\infty] dV \right) + \int_{CS} \rho (s - s_\infty) (\vec{v}_{rel.} \cdot \hat{n}) dA - \int \frac{d\dot{Q}}{T} \quad (2.23)$$

The Gouy-Stodola theorem [10] states that in any open system the irreversibility of the said system is equal to the entropy production multiplied with the equilibrium temperature. On a per time basis this leads to

$$\begin{aligned} \dot{i} &= T_\infty \dot{\Pi} \\ &= T_\infty \left[\frac{d}{dt} \left(\int_{CV} \rho [s - s_\infty] dV \right) + \int_{CS} \rho (s - s_\infty) (\vec{v}_{rel.} \cdot \hat{n}) dA - \int \frac{d\dot{Q}}{T} \right], \end{aligned} \quad (2.24)$$

which quantifies generation of new inaccessible energy on a power unit basis. This term is only zero, similar to the entropy production rate, for a reversible process. For any other process, i.e. an irreversible process, it must be positive.

By rewriting the equation it is possible to have the integrals containing entropy as separate terms on the right-hand side. Moreover, if the reference system is chosen to be moving with the control volume and a control volume is considered whose open surfaces do not move relative the reference frame, the relative velocity can be re-written to an absolute velocity. This leads to

$$\dot{i} + \int \frac{T_\infty}{T} d\dot{Q} = \frac{d}{dt} \left(\int_{CV} \rho T_\infty [s - s_\infty] dV \right) + \int_{CS} \rho T_\infty (s - s_\infty) (\vec{v} \cdot \hat{n}) dA, \quad (2.25)$$

which will be useful to construct the open system per time unit formulation of exergy.

2.2.3 Combining the First and Second Law of Thermodynamics

A mass specific measure of exergy is formed when assessing the difference in total specific energy to the specific inaccessible energy. This is not a thermodynamic function of state; rather, it shall be seen as the work potential of said amount of mass. In an open system formulation as illustrated in Eq. 2.7 this is formed when combining the difference in specific total enthalpy to the equilibrium conditions and difference in specific entropy to equilibrium conditions multiplied by the equilibrium temperature, i.e. the ambient temperature, which reads

$$\underbrace{\varepsilon}_{\text{Work potential}} = \underbrace{\Delta h + \frac{\|\vec{c}\|^2}{2}}_{\text{Total energy}} - \underbrace{T_\infty \Delta s}_{\text{Inaccessible energy}} \quad . \quad (2.26)$$

where $\|\vec{c}\|$ is the absolute magnitude of the velocity relative the atmosphere at rest.

For any system the calculation of exergy associated with a certain mass particle is also dependent on the circumstances surrounding it, e.g. if the mass particle is enclosed in a closed volume or if it is open to the surroundings. The open system as presented above thus includes the pressure-volume term, via the use of enthalpy rather than internal energy, whereas exergy for a completely closed system with rigid walls would not. Here it can be noted that the use of Gibbs free energy and Helmholtz free energy that respectively put a measure of the obtainable work for an open or closed system, is analogous to the use of exergy.

To further illustrate the point about the obtainable work potential, any work that is required for the system to find its equilibrium with the surroundings must be compensated for, under isentropic conditions, in the specific exergy term. For example, when a system is enclosed in a piston chamber the required pressure-volume work under isentropic conditions to push the piston into pressure equilibrium is subtracted from the open system formulation above to obtain the specific work potential for said system.

To construct an open system formulation of exergy the first and second law of thermodynamics formulations, expressed respectively by Eq. 2.16 and Eq. 2.25, can be combined. Arranging so that the specific exergy terms are collected on the right-hand side yields:

$$\begin{aligned} \dot{Q} - P_S - P_T - P_{\text{sys. change}} - \dot{I} - \int \frac{T_\infty}{T} d\dot{Q} = \\ \frac{d}{dt} \left(\int_{\text{CV}} \rho \left[h - h_\infty + \frac{\|\vec{c}\|^2}{2} \right] dV \right) - \frac{d}{dt} \left(\int_{\text{CV}} \rho T_\infty [s - s_\infty] dV \right) \\ + \int_{\text{CS open}} \rho \left(h - h_\infty + \frac{\|\vec{c}\|^2}{2} \right) (\vec{v} \cdot \hat{n}) dA - \int_{\text{CS}} \rho T_\infty (s - s_\infty) (\vec{v} \cdot \hat{n}) dA \end{aligned} \quad (2.27)$$

The shaping of the irreversibility expression is continued by using the specific total enthalpy and specific entropy to form the specific exergy, detailed in Eq. 2.26, and by combining the heat flow terms into one term. In addition, arranging the terms so that the irreversibility is left alone on the left-hand side yields

$$\dot{I} = \underbrace{- \int_{\text{CS open}} \rho \varepsilon (\vec{v} \cdot \hat{n}) dA - P_S - P_T + \int \frac{T - T_\infty}{T} d\dot{Q}}_{\text{steady state part}} - \underbrace{\frac{d}{dt} \left(\int_{\text{CV}} \rho \varepsilon dV \right) - P_{\text{sys. change}}}_{\text{transient part}} \quad (2.28)$$

By assuming steady state and a finite number of one-dimensional in- and outflows the formulation alters to

$$\dot{I} = \left(\sum_i \dot{m}_i \epsilon_i \right)_{\text{in}} - \left(\sum_i \dot{m}_i \epsilon_i \right)_{\text{out}} - P_S - P_T + \sum_i \int_{\text{start}}^{\text{end}} \frac{T - T_\infty}{T} d\dot{Q}_i, \quad (2.29)$$

which was presented in Eq. 2.2.

The energy terms from the first law are conserved in the expression. Only the second law contributes to the irreversibility. The irreversibility detailed for the second law, presented in Eq. 2.24, is quantifying the lost work potential in the exergy equation. Three interesting aspects of exergy analysis can be directly related to this expression. The first and primary observation is that the irreversibilities, or destruction of exergy, on a power unit is nothing but the entropy production multiplied with a reference temperature. No additional insight is needed of the underlying exergy loss sources than from what is known from entropy production. Secondly, by knowing the difference in entropy and the heat transfer for a control volume is enough to calculate the irreversibility of the said control volume. Thirdly, monitoring and analyzing entropy production is a common method for aero engine turbomachinery component analysis. Such analysis can be seen as nothing but an implicit use of the exergy methodology as the entropy production term is directly related to the irreversibility through the multiplication with a reference temperature.

The exergy balance equation in Eq. 2.2, 2.28 & 2.29 needs further explanation of the included terms. The thrust power term, the heat transfer term, and the specific exergy equation are detailed below. The shaft power is simply the work per unit time from a mechanical shaft, i.e. angular velocity multiplied with torque. Quantifying of losses in propulsion unit components that only include work terms is made by equating the lost power to the irreversibility. This is also valid for electrical components that within a propulsion unit analysis also are lumped into specific power terms. Therefore, the irreversibility of a shaft equals the difference between the input and output of shaft power. A generator irreversibility is quantified as the difference between the input shaft power to the generated electric power, whereas the opposite case is valid for an electric engine. Irreversibilities within electric circuits are likewise to the shaft handled by assessing the difference between the input to the output of power, nevertheless, in this case, the power is in an electrical form. However, if lost power within these aforementioned types of

components, that by different mechanisms, i.e. friction and electrical resistance, break down into heat, can be used to something useful within a different component, a heat exergy term can be included in the analysis that balance the irreversibility between the particular component and the connecting component.

The thrust power term can directly be rewritten as

$$P_T = \int_{CS_{\text{open}}} \rho \left(\frac{V^2}{2} - \frac{C^2}{2} \right) (\vec{v} \cdot \hat{n}) dA, \quad (2.30)$$

where V and C are the velocity magnitudes of the vector velocity relative the propulsion unit, \vec{v} , and the vector velocity relative atmosphere at rest, \vec{c} , respectively. The velocity of the propulsion unit relative to the atmosphere at rest is denoted \vec{u} for the vector quantity and U for the magnitude. It can be noted that U is equivalent to the true airspeed. To get the ground speed, the wind speed has to be compensated for. These three velocities relates by $\vec{c} = \vec{u} + \vec{v}$ as illustrated for a control volume face in Fig. 2.2, in which the angle between \vec{v} and \vec{u} is denoted with ϕ .

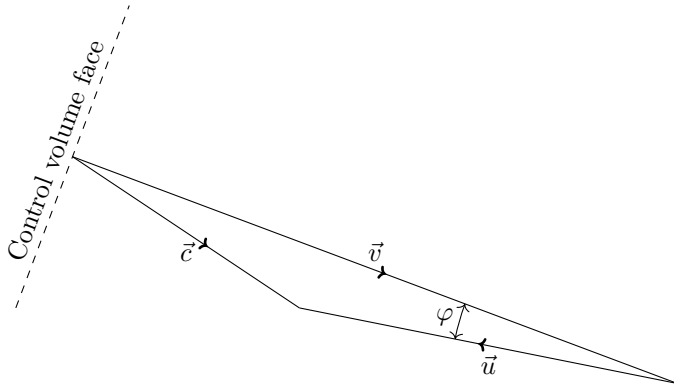


Figure 2.2: Definition of the velocities applying to a control volume face of propulsion unit

By using the relation between the velocities in combination with the assumption of a finite number of one-dimensional in- and outflows the expression can be simplified further.

$$P_T = \left(\sum_i \dot{m}_i \left[\frac{C_i^2}{2} - \frac{V_i^2}{2} \right] \right)_{\text{in}} - \left(\sum_i \dot{m}_i \left[\frac{C_i^2}{2} - \frac{V_i^2}{2} \right] \right)_{\text{out}} \quad (2.31)$$

The relation of the velocities detailed in Fig. 2.2 and use of the cosine law yield $C^2 - V^2 = U^2 - 2UV \cos \phi$. By using this identity and at the same time splitting the terms into one steady state and one transient part leads to the following thrust power term:

$$\begin{aligned}
P_T = U & \left(\overbrace{\left(\left[\sum_i \dot{m}_i V_i \cos \varphi_i \right]_{\text{out}} - \left[\sum_i \dot{m}_i V_i \cos \varphi_i \right]_{\text{in}} \right)}^{\text{steady state part}} \right. \\
& \left. + \underbrace{\left(\left[\sum_i \dot{m}_i \right]_{\text{in}} - \left[\sum_i \dot{m}_i \right]_{\text{out}} \right)}_{\text{transient part}} \right) \frac{U^2}{2} \quad (2.32)
\end{aligned}$$

If \vec{v} and \vec{u} are approximately parallel, further simplifications can be made. By defining C in the same direction as U , a new relation between the velocities is obtained ($C = U - V$). Under the assumption of parallel velocities and that steady state conditions apply, the expression simplifies to

$$P_T = U \left(\left[\sum_i \dot{m}_i V_i \right]_{\text{out}} - \left[\sum_i \dot{m}_i V_i \right]_{\text{in}} \right). \quad (2.33)$$

By studying the energy equation in Eq. 2.15, which the exergy equation depends on as shown by Eq. 2.27 - 2.28, it can be noted that the irreversibility does only depend on the magnitude of V and not C . The velocity relative to the atmosphere at rest is only added and subtracted to the original formulation to form the specific exergy integral and the thrust power term. Moreover, system performance analysis is made with a frame of reference fixed to the propulsion unit, and thus, the velocities relative the atmosphere at rest are calculated from the velocities relative the propulsion unit, and not vice versa. Hence, the assumption of \vec{c} being parallel to \vec{v} so that $C = U - V$ does not have any influence on the magnitude of the component irreversibility. Additionally, when summing the thrust power terms from several sequentially connected control volumes, all internal faces cancel out. Therefore, only the first and last faces influence the power thrust calculations under steady-state conditions. To read more about how to compensate for a potential misalignment between the thrust vector and the flight trajectory the reader is referred to Sec. 3.2.

If the exhaust nozzle of the engine is choked, then the pressure difference to the ambient conditions also contributes to the thrust power. A control volume is now considered that starts at the nozzle exit and stretches far enough to reach the ambient conditions. Using a reference frame fixed to the atmosphere at rest and looking at the pressure power term in Eq. 2.13 results in the pressure power contribution to the thrust power. The positive direction is chosen as the direction of the flow since this yields the thrust that is directed backward so that the engine is pushed forward. If the coordinate system is one-dimensional and aligned with the mass flow, the absolute velocity is $-C$ and the relative V . This yields the following expression:

$$P_{T_{\text{exhaust} \rightarrow \infty}} = \sum_i U A_{\text{nozzle-exit},i} (p_{\text{exhaust},i} - p_{\infty}). \quad (2.34)$$

Summation of the thrust power terms for each component control volume j included in the propulsion unit, including the exhaust "component", during steady state yields

$$P_{T\text{prop. unit}} = \sum_j P_{T,j} = U \left(\left[\sum_i \dot{m}_i V_i \right]_{\text{exhaust}} - \left[\sum_i \dot{m}_i V_i \right]_{\text{intake}} \right) + U \left(\sum_i A_{\text{nozzle-exit},i} [p_{\text{exhaust},i} - p_\infty] \right), \quad (2.35)$$

which is equal to the net thrust multiplied by the flight velocity. This expression constitutes the thrust work per unit time of the propulsion unit and makes up the useful thrust power term included in Eq. 2.5 for calculation of the rational efficiency.

The velocity in the exhaust is here taken as the propulsion unit axial component of the true velocity and the mass flow as the true mass flow. This would be equal to compensating the ideal mass flow rate with a discharge coefficient as the one-dimensionally effective nozzle area is smaller than the geometric area due to a build-up of a side-wall boundary layer. To obtain the true velocity requires the multiplication of the ideal velocity by a velocity coefficient that compensates for the viscous losses in the expansion. Additionally, to obtain the axial component of the velocity both the potential swirl and the tangentially independent part of the radial velocity both need to be compensated for. The former loss is however not generally considered in performance studies as the optimum is a flow without swirl, and additionally, to calculate the swirl component requires designing the turbomachinery components and other components that have a turning capability, e.g. turbofan turbine exhaust casing. The latter loss becomes important for convergent-divergent nozzles as the flow also expands radially outwards in the divergent part of the nozzle. In case of a convergent-divergent nozzle, this loss can be compensated for using a coefficient of angularity.

For here on focus the shifts towards explaining the heat transfer integral in the irreversibility equation (Eq. 2.16 and Eq. 2.25) into further detail. First of all, it shall be mentioned that heat transfer can occur in three different ways; conduction, convection and thermal radiation. Whereas conduction and convection travel through and by matter, radiation travels by photon rays between matter. For a control volume formulation, this leads to some differences when it comes to the exergy of heat. Heat transfer in a control volume formulation has two contributing terms; fluxes over the control volume surface by conduction and body heating by radiation, which can be seen in Eq. 2.36. The advection part of convective heat transfer, i.e. transport of heat by fluid flow, is already accounted for in the mass flux terms.

$$\dot{Q} = \int_{\text{CS}} \vec{\phi}_q \cdot \hat{n} dA + \int_{\text{CV}} \rho \dot{q} dV \quad (2.36)$$

The heat transfer exergy integral shares origin from both the conservation of energy and the entropy equation, where the conservation of energy yields the total heat energy and the

entropy equation contributes the inaccessible heat energy. The term is dependent on the static temperature at which the heat transfer occurs. Thus, it reflects that heat is losing quality when exchanged to a lower temperature medium. This is motivated from heat transfer being dependent on a temperature gradient as the driving force, leading to that heat transfer is no longer possible when the temperature of the heat source has become equal to its surrounding temperature. The formulation, without any simplifications, is

$$\int \frac{T - T_{\infty}}{T} d\dot{Q}. \quad (2.37)$$

The similarity between the heat exergy term above and the Carnot's efficiency for a heat cycle, is striking, as the same temperature fraction as found when equating T to T_H and T_0 to T_L in the heat transfer exergy term.

As the heat transfer exergy term is dependent on the static temperature at which the heat transfer occurs it means that the flux term and the body heating terms must be treated slightly differently. The temperature at which the heat transfer occurs for the flux term is the temperature at the boundary. On the other hand, for the body heat term, it is instead the temperature of the matter emitting and absorbing the radiation.

It can be noted that thermal radiation is often seen as a surface phenomenon even though it is a volumetric phenomenon related to matter. For gases or semi-transparent liquids or solids, the radiation should be considered volumetric. However, neighboring particles absorb radiation heavily within opaque liquids and solids. Thus, the radiation from these materials originate from closest micrometers to the surface which leads to radiation often being considered as a surface phenomenon. In this case, the temperature of these surface layers is considered as the temperature at which the heat transfer occurs in the exergy assessment.

Interaction of radiation with matter is, however, an inherently irreversible and thus, entropy producing process [16]. Therefore, for radiation, contrary to conduction, a modified heat exergy term is needed. According to Petela, when assuming constant temperature and a black or grey body the obtainable work, i.e. exergy, from radiation relates to the radiation internal energy by the following fraction [17, 18]:

$$\frac{E_{x,\text{rad.}}}{E_{\text{rad.}}} = 1 + \frac{1}{3} \left(\frac{T_0}{T} \right)^4 - \frac{4}{3} \left(\frac{T_0}{T} \right) \quad (2.38)$$

It can also be noted that other scholars have made other suggestions. However, on the basis of relating the obtainable work from an energy stream, the Petela formulation aligns the best with the exergy methodology of this thesis. Bejan reviewed three different suggestions, including one of them being Petela's formulation, and argued that all are correct even though they yield different results [19]. Nevertheless, this position is something that Petela objects against [18]. An alternative to Petela's formulation was posed by Spanner and suggested to measure the radiation exergy as the absolute work instead

of the obtainable work [20]. Moreover, a third option is to relate radiation heat to the obtainable useful work, which was proposed by Jeter [21]. The first of the alternatives fall short on putting a limit to the obtainable work. The second alternative is identical to the term for conduction, meaning that the interaction with matter is not included.

For analysis of hot surfaces in propulsion units emitting heat to the surroundings, the system boundary can be defined to only include conduction within the solid material connecting to the radiation emitting surface. In this sense, the option of how to treat heat radiation exergy does not pose an influence on the analysis as the surface irreversibility and the radiation irreversibility can be combined into one term. The same thing would be valid when the propulsion unit is heated by thermal radiation from a very hot exhaust as such found in rockets or jet engines with afterburners. For all practical matters surrounding current commercial aircraft engines, this becomes a viable path without having to consider which analysis to follow. In fact, this procedure is equivalent to the Jeter's formulation. However, for solar powered aircraft such as demonstrated in Airbus Zephyr, NASA Pathfinder, NASA Pathfinder Plus, NASA Centurion, NASA Helios, Solar Impulse 1 and Solar Impulse 2 it would be beneficial for the analysis to include radiation heat exergy as this allows for an analysis measuring the irreversibility between the rays of the sun to the surface of the solar power panels, including both the reflection at the surface and entropy production of said surface.

The usage of the heat exergy term when radiation is not considered it also non-trivial. When handling control volumes with heat transfer over the system boundary, the exergy heat transfer term needs further attention. It would be possible to integrate the term numerically if a computational representation existed of the static temperature and the heat transfer rate through the control surface. The existence of such a representation is, however, not the case in existing performance codes. Without a detailed knowledge of the heat transfer process, the heat exergy flux term in Eq. 2.2 needs, therefore, to be simplified before implementation into an aero-engine performance code.

Consider a mass particle moving along the control volume surface and being heated/cooled by $d\dot{Q}_i$ that crosses the boundary. When it is possible to assume constant specific heat, using $d\dot{Q}_i = c_{p,i} \dot{m}_i dT_{0i}$ and $\dot{Q}_i = c_{p,i} \dot{m}_i (T_{0i,end} - T_{0i,start})$, the heat transfer integral can be rewritten,

$$\begin{aligned} \sum_i \int_{start}^{end} \frac{T - T_\infty}{T} d\dot{Q}_i &= \sum_i \frac{d\dot{Q}_i}{dT_{0i}} \int_{T_{i,start}}^{T_{i,end}} \frac{T - T_\infty}{T} dT_{0i} \\ &= \sum_i \frac{\dot{Q}_i}{T_{0i,end} - T_{0i,start}} \int_{T_{i,start}}^{T_{i,end}} \frac{T - T_\infty}{T} dT_{0i}. \end{aligned} \quad (2.39)$$

If the velocities are low or alternatively constant during the heat transfer, so that $T_{0i,end} - T_{0i,start} = T_{i,end} - T_{i,start}$ and $dT_{0i} = dT_i$, the following simplification can be

made,

$$\begin{aligned}
\sum_i \int_{\text{start}}^{\text{end}} \frac{T - T_\infty}{T} d\dot{Q}_i &= \sum_i \frac{\dot{Q}_i}{T_{i,\text{end}} - T_{i,\text{start}}} \int_{T_{i,\text{start}}}^{T_{i,\text{end}}} \frac{T - T_\infty}{T} dT_i \\
&= \sum_i \frac{\dot{Q}_i}{T_{i,\text{end}} - T_{i,\text{start}}} \left(\begin{array}{c} T_{i,\text{end}} - T_{i,\text{start}} \\ -T_\infty (\ln [T_{i,\text{end}}] - \ln [T_{i,\text{start}}]) \end{array} \right) \\
&= \sum_i \dot{Q}_i \left(1 - T_\infty \frac{\ln [T_{i,\text{end}}/T_{i,\text{start}}]}{T_{i,\text{end}} - T_{i,\text{start}}} \right). \tag{2.40}
\end{aligned}$$

Alternatively, if the Mach number rather than the velocity is constant during the heat transfer, so that $T_{0i,\text{end}} - T_{0i,\text{start}} = (T_{i,\text{end}} - T_{i,\text{start}}) \cdot (1 + \frac{\gamma-1}{2} M^2)$ and $dT_{0i} = dT_i \cdot (1 + \frac{\gamma-1}{2} M^2)$, the same simplifications can be made as stated in Eq. (2.40), i.e.

$$\begin{aligned}
\sum_i \int_{\text{start}}^{\text{end}} \frac{T - T_\infty}{T} d\dot{Q}_i &= \sum_i \frac{\dot{Q}_i}{(T_{i,\text{end}} - T_{i,\text{start}}) \cdot (1 + \frac{\gamma-1}{2} M^2)} \\
&\quad \cdot \int_{T_{i,\text{start}}}^{T_{i,\text{end}}} \frac{T - T_\infty}{T} \left(1 + \frac{\gamma-1}{2} M^2 \right) dT_i \\
&= \sum_i \dot{Q}_i \left(1 - T_\infty \frac{\ln [T_{i,\text{end}}/T_{i,\text{start}}]}{T_{i,\text{end}} - T_{i,\text{start}}} \right). \tag{2.41}
\end{aligned}$$

If the temperature is or can be approximated as constant during the heat transfer process, the integral in Eq. (2.2) can be simplified,

$$\sum_i \int \frac{T - T_\infty}{T} d\dot{Q}_i = \sum_i \dot{Q}_i \frac{T_i - T_\infty}{T_i} \tag{2.42}$$

The simplified term with a constant temperature showed in Eq. 2.42 was included by previous authors as the heat transfer exergy term in the governing irreversibility equation without the statement of the necessary assumptions to do so [1]. It is noted that the expression in Eq. 2.42 is consistent when taking the limit of Eq. 2.40 and 2.41. Moreover, it is also noted that this expression would only be valid for an evaporating or condensing fluid. Equation 2.42 can however also be considered a valid approximation for heat transfer with a very low temperature difference per total heat transfer rate.

The specific exergy introduced in Eq. 2.26 needs further attention before implementation into a performance code. The specific exergy includes the different forms of exergy that are applicable to a flying aero engine, i.e. a physical part and a chemical part. The physical component can, in turn, be divided into several terms; thermomechanical, kinetic and potential energy. Since the use of the separated terms more clearly describes each term's origin it is the preferred convention in this work. The potential energy for the gas mass flow can be neglected.

$$\varepsilon = \varepsilon_{\text{thermomechanical}} + \varepsilon_{\text{kinetic}} + \varepsilon_{\text{chemical}} \tag{2.43}$$

The thermomechanical part is different from zero as long as the temperature and pressure are different from the ambient conditions. The kinetic exergy is just the kinetic energy of the current state since the gas when brought to equilibrium with the ambient conditions will be at rest. The chemical exergy is the difference in chemical potential between the true and the equilibrium composition of species, which is the energy that can be absorbed or released in a chemical reaction or phase transition. From a thermodynamics modeling perspective the chemical component has two components; the difference in standard Gibbs free energy of formation of the individual species and the Gibbs free energy of mixing.

When an ideal gas is considered, the difference in chemical potential is only dependent on the entropy of mixing. For a gas composition with only species that only exist in the equilibrium state, there will be no chemical exergy of formation difference between the species of the true and the equilibrium conditions. The specific exergy equation applied to aero engine for such gas is

$$\varepsilon = \underbrace{h - h_{\infty} - T_{\infty}(s_{th.} - s_{th.,\infty})}_{\text{Thermomechanical}} + \underbrace{\frac{C^2}{2}}_{\text{Kinetic}} + \underbrace{T_{\infty}(s_{mixing} - s_{mixing,\infty})}_{\text{Chemical}}. \quad (2.44)$$

The thermomechanical term includes entropy contributions denoted with the suffix "th" for thermomechanical, which implies that the mixing effect is not included in the term. Even so, the thermomechanical entropy terms can also be taken as the respective true entropy value for the true gas composition since the mixing entropy contributions to both entropy terms cancel out each other from equal gas compositions. The mixing entropy forming the chemical exergy term in Eq. 2.44 originate from different partial pressures compared to the ambient conditions. Dalton's law states that the partial pressure is proportional to the mole fraction. Only the gas downstream of the combustion will have different gas proportions than the ambient conditions and consequently the chemical exergy term will only be different from zero after the combustion has taken place. This chemical exergy term can be seen as the work that can be obtained after the gas expanded reversibly to the pressure of the environment by letting the gas discharge reversibly via a semi-permeable membrane to each species' respective partial pressure.

The total entropy of mixing on a joule per kelvin unit associated with the mixing of the gas composition of the ambient conditions and an amount of ideal gas flow mass, $m_{\text{aero engine gas}}$, that at a given moment is in an arbitrary component downstream of the combustion process, can be calculated via

$$\Delta S_{\text{mixing}} = \left(\underbrace{\left[-m \sum_i y_i R_i \ln x_i \right]_{\text{aero engine gas}} + \left[-m \sum_i y_i R_i \ln x_i \right]_{\text{ambient air}}}_{\text{before mixing}} \right) - \left(\underbrace{\left[-m \sum_i y_i R_i \ln x_i \right]_{\text{aero engine gas}} + \left[-m \sum_i y_i R_i \ln x_i \right]_{\text{ambient air}}}_{\text{after mixing}} \right), \quad (2.45)$$

where R is the specific gas constant, and y and x corresponds to the mass- and mole fraction, respectively. Since mass is conserved between the states the formulation can be altered to:

$$\Delta S_{\text{mixing}} = \left(-m \sum_i y_i R_i \ln \frac{x_{\text{before mixing},i}}{x_{\text{after mixing},i}} \right)_{\text{gas aero engine}} + \left(-m \sum_i y_i R_i \ln \frac{x_{\text{before mixing},i}}{x_{\text{after mixing},i}} \right)_{\text{ambient air}} \quad (2.46)$$

We assume that the ambient conditions stretch significantly far away that the composition after mixing of the aero engine gas flow mass and the ambient conditions are no different from the initial composition at the ambient conditions, i.e. the ambient air is the equilibrium state. For the gas flow aero engine terms this brings the following change:

$$\Delta S_{\text{mixing}} = \left(-m \sum_i y_i R_i \ln \frac{x_{\text{before mixing},i}}{x_{\infty,i}} \right)_{\text{aero engine gas}} + \left(-m \sum_i y_i R_i \ln \frac{x_{i,\text{before mixing}}}{x_{\text{after mixing},i}} \right)_{\text{ambient air}} \quad (2.47)$$

When considering the specific exergy associated with the engine gas flow it implies that the upper row of the formula is considered, it is

$$\Delta s_{\text{mixing, aero engine gas}} = - \sum_i y_i R_i \ln \frac{x_i}{x_{\infty,i}}.$$

This can be introduced in the specific exergy equation to form

$$\varepsilon = \underbrace{h - h_{\infty} - T_{\infty}(s_{\text{th.}} - s_{\text{th.,}\infty})}_{\text{thermomechanical}} + \underbrace{\frac{C^2}{2}}_{\text{kinetic}} + T_{\infty} \underbrace{\left(\sum_i y_i R_i \ln \frac{x_i}{x_{\infty,i}} \right)}_{\text{chemical}}. \quad (2.48)$$

The ambient relative humidity needs to be set different from zero, to allow for proper exergy calculations, when using Eq. 2.48 as the chemical term relies on the exhaust species to also exist in the equilibrium conditions. The water vapor content varies strongly dependent on geography and time of the year, produced mainly from evaporated sea water, and plant transpiration. According to Szargut the reference humidity for exergy calculations is 0.7% [22]. However, aero-engine performance simulations are commonly made using zero relative humidity. Moreover, unburned fuel, dissociation combustion products, and sulfur dioxide, from the combustion of sulfur-containing fuel, are also not present in the equilibrium conditions. As previously explained in the derivation of the mixing exergy above this is because the ambient conditions are assumed to stretch far enough so that the different gas composition in the engine will not affect the surroundings. It shall be noted that the mixing entropy for the total assessment of both the aero engine gas mass and ambient air mass would effectively be zero in Eq. 2.47. Using the assumption that the ambient conditions stretches far enough to be unchanged after mixing also leads to the consequence that $m_{\text{aero engine gas}}/m_{\text{ambient air}}$ becomes infinitely small which cancels the aero engine gas term as $\lim_{\xi \rightarrow 0} \xi \ln(\xi) = 0$ for an arbitrary variable ξ .

Szargut described a way of calculating chemical exergy for non-environmental resource species by ascribing them as a combination of environmental species [23]. The formulation is here altered to be based on a joule per kilo basis. For an ideal gas one gets

$$\begin{aligned} \varepsilon_{\text{chemical}} = & \left[\sum_i y_i \Delta g_{f,i}^\circ \Big|_{T_\infty} + T_\infty \sum_i y_i R_i \ln x_i \right]_{\text{resource species}} \\ & - \left[\sum_j \sum_i \left(\Delta g_{f,i}^\circ \Big|_{T_\infty} + T_\infty R_i \ln x_{\infty,i} \right) \zeta_{j,i} \right]_{\text{environment species}} \end{aligned} \quad (2.49)$$

where Gibbs free energy of formation is obtained by $\Delta g_{f,i}^\circ \Big|_{T_\infty} = \Delta h_{f,i}^\circ - T_\infty \Delta s_{f,i}^\circ$. The summation of environmental species transforms the resource species of index j to the environmental species of index i . The mass fraction of environmental species per unit of resource species is calculated by $\zeta_{j,i} = y_j \frac{\nu_{i,j}}{\nu_j} \frac{M_i}{M_j}$, where ν represents the stoichiometric coefficient for a reaction that transforms the resource species to a environmental species. It can be noted that Eq. 2.49 reduces to Eq. 2.48 for a gas with only environmental species, as the heat of formation terms negate each other.

Carbon monoxide using oxygen to gain carbon dioxide can be used as an example. For this reaction the resource stoichiometric coefficient ν_{CO} becomes 2 and the environmental stoichiometric coefficient ν_{CO_2} and ν_{O_2} to 2 and -1, respectively, as the reaction can be written as $2\text{CO} \rightarrow 2\text{CO}_2 - \text{O}_2$.

The same formula as detailed in Eq. 2.49 may also be used for liquids when ideal solutions are considered, meaning that Raoult's law is valid. When real solutions are considered the mixing terms need to be altered using an activity coefficient, γ_i , for each species. The

updated mixing term then becomes:

$$T_\infty \sum_i y_i R_i \ln \gamma_i x_i \quad (2.50)$$

It has previously been suggested to include stable species in the atmosphere, hydrosphere, and lithosphere to define standard chemical exergy [22, 23]. This calculation is dependent on the concentration levels in the respective environment. The reference species in the atmosphere is the species in normal composition of air including N₂, O₂, CO₂, H₂O, Ar, He and Ne. Other species can generally both be referenced to the composition of seawater or the earth's crust, which for many elements give similar results [23]. The concentration of many elements within seawater is known with sufficient accuracy which yields relatively high precision. However, some elements show a considerable deviation from thermodynamic equilibrium between being dissolved in sea water and as solid components. In these case, the solid reference species are recommended to be used. For sulfur, which has been mentioned previously, referencing to sea water and the earth's crust gives similar results.

Having a reference from a different environment from where the application resides implies that work that can be obtained from a different composition to the equilibrium state is evaluated when the element has reached this other environment reversibly. The applicability of this point of view can be debated but will at least allow for chemical exergy calculation including these non-atmospheric species.

As previously described having a relative humidity to zero would eliminate the water vapor content of the air. Using a different reference than the ambient environment consequently leads to that ambient air has obtainable work, which from a physical point of view is questionable. Therefore, Szargut's method yields little help for water vapor as long as it is seen as an atmospheric gas. It would be possible, although, quite unorthodox, to stop considering water vapor as an atmospheric gas and instead relate it to seawater by use of the Gibbs free energy of vaporization. However, at that point one could equally envision another atmospheric environment with the relative humidity of 0.7%, as suggested by Szargut, that would be closer to the ambient conditions of the engine.

Unburned fuel can be handled using Eq. 2.49 as long as a way is devised to relate all combustion products to environmental species. Completely unburned fuel in the exhaust still has the same chemical exergy as initially calculated for the fuel. For more about calculating the exergy of fuel the reader is referred to Sec. 2.3. Likewise is valid for incomplete combustion and dissociation products during combustion, as only elements from the fuel and the environment can react.

For a discussion of when and how the chemical mixing exergy can be omitted the reader is referred to Sec. 2.3.2.

2.3 Fuel Exergy

Fuel exergy is equivalent to the work potential found between the state of unburned fuel and the state when burned fuel and the reference environment are in complete equilibrium with each other. During the combustion process, the species in the fuel mixture react with oxygen, and other new species are formed while the difference in enthalpy of formation is released as heat. The chemical component in the standard exergy equation described in Eq. 2.48 originates from the entropy of mixing and not the chemical reaction. A method that can be used to evaluate exergy during a chemical reaction, by including the release of enthalpy and entropy locked in the chemical composition, is described in detail by Kotas [24]. This method is also consistent when Eq. 2.49 is used to evaluate chemical exergy with everything else similar to Eq. 2.48. The exergy from potential exergy is omitted, likewise to the calculation of ideal gas exergy. The equation is

$$\varepsilon_{\text{fuel}} = \varepsilon_{\text{fuel,thermomechanical}} + \varepsilon_{\text{fuel,kinetic}} + \varepsilon_{\text{fuel,chemical}}, \quad (2.51)$$

where the subcomponents are calculated by the following formulas

$$\begin{aligned} \varepsilon_{\text{fuel,thermomechanical}} &= \left(\sum_i \beta_i [h_i - h_{\text{ss},i}] - \sum_i \lambda_i [h_{\infty,i} - h_{\text{ss},i}] \right) \\ &\quad - T_{\infty} \left(\sum_i \beta_i [s_i - s_{\text{ss},i}] - \sum_i \lambda_i [s_{\infty,i} - s_{\text{ss},i}] \right), \\ \varepsilon_{\text{fuel,kinetic}} &= \sum_i \beta_i \frac{C_i^2}{2} \text{ and} \\ \varepsilon_{\text{fuel,chemical}} &= \sum_i (\beta_i - \lambda_i) \cdot (\Delta h_{\text{f},i}^{\circ} - T_{\infty} \Delta s_{\text{f},i}^{\circ}) \\ &\quad + T_{\infty} \left(\left[\sum_i \beta_i R_i \ln \frac{\beta_i M_i}{\sum_j \beta_j M_j} \right] - \left[\sum_i \lambda_i R_i \ln x_{\infty,i} \right] \right), \end{aligned} \quad (2.52)$$

of which β_i = mass proportion of constituent i in fuel,
 λ_i = mass of combustion product of constituent i per unit burned fuel,
 $\Delta h_{\text{f},i}^{\circ}$ = standard enthalpy of formation for constituent i and
 $\Delta s_{\text{f},i}^{\circ}$ = standard entropy of formation for constituent i .

It is worth noting that fuel exergy is not identically equal to the LHV nor the HHV even though it is quite similar in magnitude to the heat of combustion. According to Szargut LHV and fuel exergy are almost equal for most hydrocarbons [22]. Fuel exergy, as opposed to LHV and HHV, does also include a couple of additional contributing terms aside from the heat of combustion. The heat of combustion is calculated as the difference of heat of formation between the products and the reactants. The heat of formation is

corresponding to the difference in enthalpy of a compound compared to its constituent elements at standard state temperature and pressure. This implies that it quantifies the amount of enthalpy locked into the chemical composition. The heat of combustion is included in the chemical fuel exergy term as the summation of the heat of formation terms. The entropy of formation is, in addition to the heat of formation, also included in the chemical fuel exergy term. This term reflects upon the case that entropy for the species after a combustion is much larger than the for the reactants, i.e. heat is captured by the products. Chemical mixing exergy is also included in the chemical exergy term. For a fuel mixture that cannot be considered an ideal material, i.e. not an ideal gas or solution, the mixing must be compensated for by a fugacity quantity or an activity coefficient, respectively. Typically, the chemical fuel exergy term is much larger than the thermomechanical fuel exergy, and the heat of combustion constitutes the dominating part of the chemical fuel exergy.

It could be questioned whether it would be the most accurate to use LHV or HHV to assess the heat of combustion. The difference between LHV and HHV is the heat of vaporization, where the first heating value considers any formed water during combustion as vapor as opposed to the latter where a liquid is assumed. The appropriate choice for the heat of combustion term is dependent on whether the ambient conditions implies that the air is saturated with vapor or not. In case of ambient conditions including air saturated with vapor the water formed during the combustion process will condense when brought to equilibrium with its surroundings, whereas if the relative humidity instead is lower than 100% the same exhaust water will remain as vapor. Aero engine performance simulations are usually made at a low relative humidity, and thus LHV is the appropriate choice. Using the enthalpy of formation for water as vapor is also consistent with the implementation by Horlock and Clark [1].

The difference in enthalpy and entropy when comparing the thermomechanical state of the fuel at rest to the ambient conditions for the combustion products is included in the thermomechanical term. This term reflects upon the work potential inherently present in the different pressure and temperature for the unburned fuel compared to the ambient conditions. The kinetic exergy is left unchanged compared to the standard formulation expressed in Eq. 2.48 as the change of species between the true conditions and the reference does not affect the term.

The method described in Eq. 2.51 to calculate fuel exergy requires full knowledge of the fuel composition. Jet propulsion fuel, or more specifically Jet A in the case of commercial aviation, is a mixture of various hydrocarbons which therefore becomes less straightforward to model. However, even without knowledge of the full composition, it is possible to a large extent to make use of what is commonly included in many engine performance modeling tools. The heat of combustion term in the chemical fuel exergy can be quantified as the LHV value for the specific fuel mixture.

The thermomechanical enthalpy contribution from the fuel can be assessed using the temperature dependent tables that are included to incorporate the fuel energy difference

corresponding to a fuel temperature different from the standard state temperature. Enthalpy is not dependent on pressure for liquids, and therefore the effect of a different pressure than the standard state does not need to be incorporated in the analysis. Entropy of formation nor entropy temperature tables are neither on the other hand not commonly available in the aero engine performance codes. The combustion modeling code Chemical Equilibrium and Applications [25], developed by NASA, is using $C_{12}H_{23}$ as representative of Jet A. Hence, the fuel entropy of formation as well as fuel the thermomechanical entropy can be assumed as the values corresponding to $C_{12}H_{23}$. The post-combustion species are common substances, and can be found in a reference containing tabulated thermodynamic data [26] or be modeled using polynomials described by McBride and Gordon [25].

In the case of modeling fuel exergy of Jet A the different terms become

$$\begin{aligned}
\varepsilon_{\text{JetA,thermomechanical}} &= \left([h - h_{\text{ss}}]_{\text{fuel-table}} - \sum_i \lambda_i [h_{\infty,i} - h_{\text{ss},i}] \right) \\
&\quad - T_{\infty} \left([s - s_{\text{ss}}]_{C_{12}H_{23}} - \sum_i \lambda_i [s_{\infty,i} - s_{\text{ss},i}] \right), \\
\varepsilon_{\text{JetA,kinetic}} &= \frac{C_{\text{fuel}}^2}{2} \text{ and} \\
\varepsilon_{\text{JetA,chemical}} &= \text{LHV} - T_{\infty} \left(\Delta s_{\text{f},C_{12}H_{23}}^{\circ} - \sum_i \lambda_i \Delta s_{\text{f},i}^{\circ} \right) \\
&\quad - T_{\infty} \left(\sum_i \lambda_i R_i \ln x_{\infty,i} \right). \tag{2.53}
\end{aligned}$$

It can be noted for Eq. 2.51 & 2.53 that the calculation of fuel exergy cannot be checked later in the combustor component exergy assessment. When fuel exergy is included with the other and in- and outflows the number of variables becomes sufficient to determine the combustor irreversibility.

Fuel exergy varies with the ambient conditions, the flight velocity, and fuel conditions. To illustrate the effect from different alternations Fig. 2.3 is included. First and foremost, fuel exergy is quite similar in magnitude as the lower heating value across the various alternations. Second, it can be seen that the ISA conditions for various altitudes impose a larger difference on the fuel exergy than the other alternations, except from having a relative humidity of 75%.

The impact from a fuel with higher temperature on fuel exergy increases with altitude, as the inaccessible energy part of the thermomechanical component decreases linearly with lower ambient temperature. The velocity of the fuel is taken before it is injected into the combustor. Hence, the velocity relative to the propulsion unit is assumed to zero, which makes the velocity relative to the atmosphere at rest equal to the flight velocity. The kinetic energy is quadratically dependent on the flight mach number, and

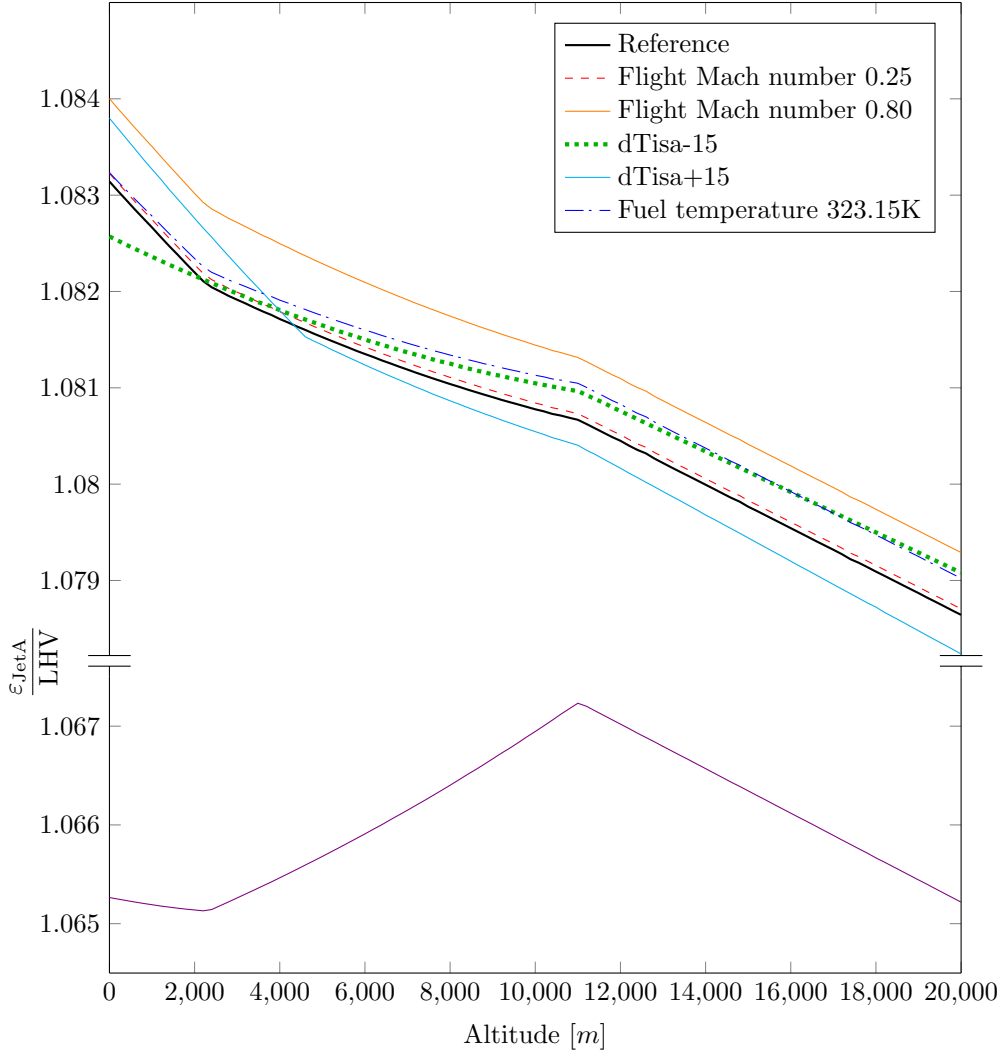


Figure 2.3: Jet A fuel exergy normalized by its lower heating value as a function of ISA [27] conditions for a certain altitude. A reference curve, illustrated in black, is included where the absolute velocity relative to the atmosphere at rest is zero, the fuel temperature is 298.15K, and the relative humidity is 0.7%. Six other curves shows the effect of a single change, and all of them are presented in the figure legend. Note that the y-axis is broken as the chemical exergy from mixing with a relative humidity of 75% impose a much larger impact on the calculations than the other alternations.

therefore, the higher mach number alternation has a much larger impact than the lower. The effect from the alternations of the ISA-temperature differ with altitude. The ambient temperature affects the thermomechanical enthalpy and entropy, all terms in Eq. 2.53 where the temperature is directly stated, and the molar composition of ambient air, which depends on the water content in the air that in turn is a function of relative humidity, ambient temperature and pressure. Thus, the less coherent impact. By increasing the water content to a relative humidity of 75% the mole fraction of the water content in the air goes from very small to less small. Water is formed during combustion, and therefore, the corresponding λ is positive. The limit of the natural logarithm of zero is negative infinity. Thus, the chemical mixing component becomes considerably larger for the a relative humidity of 0.7% than 75%. Due to the broken y-axis, the difference is also larger than the distance in the graph. Furthermore, air's ability to hold water before it becomes saturated is heavily dependent on the temperature, and hence, a larger difference compared to the reference is observed at lower altitudes.

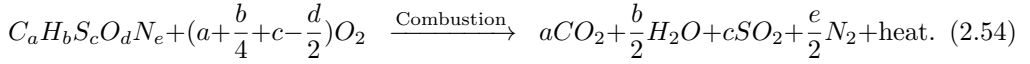
The different components of fuel exergy were also studied in additional studies, which allows herein to aid further understanding of the terms. The atmospheric temperature decreases linearly with higher altitude until the stratosphere begins at 11000 meters, after which the temperature is constant. Thus, the noticeable break in all curves. Pressure decreases logarithmically in both the troposphere and the stratosphere. Therefore, as the the fuel is further from the thermomechanical equilibrium conditions with higher elevation, the thermomechanical component of the fuel exergy increases with altitude. The chemical fuel exergy component that is additional to the lower heating value is, however, much greater than the thermomechanical part. Of this part, the mixing constitutes the major component.

2.3.1 Fuel Exergy Combustion Modeling

Combustion in the ideal circumstances balances fuel reactants with oxidants, and generate only a limited number of products, resulting from complete combustion. In a real case, it is likely that some of the fuel reactants only partially react with the oxygen during the combustion process. These elements will then consequently stay unburned or remain as non-ideal products in the exhaust flow. Combustion at very high temperatures might also cause dissociation of the reaction products, a more general formulation, in this case, is the assumption of chemical equilibrium rather than complete combustion. Both incomplete combustion as well as dissociation are resulting in lower flame temperatures than during complete combustion. Fuel exergy is no different from exergy in general as it quantifies the work potential. Hence, complete combustion must always be considered in terms of quantifying fuel exergy. This is also true in cases where the real combustion process is incomplete as well as in existence of dissociation of the combustion products. Rather than considering these irregularities as a cause for lowering the work potential they should be regarded as irreversibilities of the combustion process.

Complete combustion is assessed by balancing the number of atoms in the reactants

with the products, assuming only water and oxides of the non-hydrogen atoms among the products. Fuel can consist of many different elements, here the general case of a fuel molecule consisting of carbon, hydrogen, sulfur, oxygen, and nitrogen is considered. Among the fuel elements that react with the oxide, the following is true; carbon will yield carbon dioxide, hydrogen will yield water and sulfur will yield sulfur dioxide. Oxygen in the fuel will lower the amount of the required external oxidant. Nitrogen does not under ideal conditions yield any nitrogen oxide as the Gibbs free energy of formation is lower for the separate constituents. The general formula balancing the elements becomes



Calculating the mass proportion of a constituent in the fuel, β_i and the mass of combustion product per unit burned fuel, λ_i , for a fuel mixture consisting of multiple types of fuel molecules is possible when using the statement above for each and every one of the fuel molecules. The mass proportions of the different fuel molecules are described by $y_{\text{fuel},i}$. The expressions become:

	β_i	λ_i	
$[C_{a_1} H_{b_1} S_{c_1} O_{d_1} N_{e_1}]_1$	$y_{\text{fuel},1}$	0	
\vdots	\vdots	\vdots	
$[C_{a_n} H_{b_n} S_{c_n} O_{d_n} N_{e_n}]_n$	$y_{\text{fuel},n}$	0	
O_2	0	$-\sum_{i=1}^n y_{\text{fuel},i} \frac{M_{O_2}}{M_{\text{fuel},i}} (a_i + \frac{b_i}{4} + c_i - \frac{d_i}{2})$	
CO_2	0	$\sum_{i=1}^n y_{\text{fuel},i} \frac{M_{CO_2}}{M_{\text{fuel},i}} a_i$	(2.55)
H_2O	0	$\sum_{i=1}^n y_{\text{fuel},i} \frac{M_{H_2O}}{M_{\text{fuel},i}} \frac{b_i}{2}$	
SO_2	0	$\sum_{i=1}^n y_{\text{fuel},i} \frac{M_{SO_2}}{M_{\text{fuel},i}} c_i$	
N_2	0	$\sum_{i=1}^n y_{\text{fuel},i} \frac{M_{N_2}}{M_{\text{fuel},i}} \frac{e_i}{2}$	

Jet A consists of a mixture of many hydrocarbons that all have carbon numbers ranging between 8 and 16 [28]. The mass composition of the hydrocarbons in the fuel is however not known, which results in that the general formula from above cannot be used. Thus, another way must be found. One option could be using $C_{12}H_{23}$ as representative of Jet A in line with the combustion code Chemical Equilibrium and Applications, which previously also have been applied by the author of this thesis [7]. Another way could be looking at the mass composition of the single elements in the fuel. In the case of the general fuel molecule, this requires the mass proportions of the five elements. In case of a pure hydrocarbon the number of elements reduces to two. This approach can yield the composition of the products but it will not be useful trying to compute heat of combustion as the composition of the reactants is unknown. For Jet A it is not necessary to know

the composition of the reactants since they can be accounted for by other means in the fuel exergy assessment. In short, the LHV value and the enthalpy tables can be used in combination with the assumption that the composition of $C_{12}H_{23}$ is representative for Jet A to evaluate the less dominant entropy fuel exergy terms.

Assuming that the mass proportions of the different elements in the fuel are known the reaction products can be assessed by altering the method from above. The expressions become:

$$\begin{array}{c|c}
 & \lambda_i \\
 \hline
 \left[\begin{array}{l} C y_{\text{fuel},C} + H y_{\text{fuel},H} + S y_{\text{fuel},S} \\ + O y_{\text{fuel},O} + N y_{\text{fuel},N} \end{array} \right] & 0 \\
 O_2 & y_{\text{fuel},O} - \left(\frac{y_{\text{fuel},C}}{M_C} + \frac{y_{\text{fuel},H}}{4M_H} + \frac{y_{\text{fuel},S}}{M_S} \right) M_{O_2} \\
 CO_2 & y_{\text{fuel},C} \frac{M_{CO_2}}{M_C} \\
 H_2O & y_{\text{fuel},H} \frac{M_{H_2O}}{2M_H} \\
 SO_2 & y_{\text{fuel},S} \frac{M_{SO_2}}{M_S} \\
 N_2 & y_{\text{fuel},N}
 \end{array} \quad (2.56)$$

2.3.2 Possibility of Omitting the Chemical Mixing Exergy to Ambient Air

For all practical matters, the work that theoretically can be obtained from the different partial pressures between the composition of a gas and its environment is unobtainable for an aircraft engine. A semi-permeable membrane being able to handle the vast amount of flow passing the nozzle is likely very heavy and yield significant pressure losses at the high velocities present in an aircraft engine. Instead, as no additional functionality is likely to be devised with the intention to make use of the mixing work potential, it leads to the chemical mixing exergy being an irreversibility in the exhaust as unused work potential. Therefore, it could be argued that the chemical mixing exergy in the exhaust can be omitted for all aerospace applications. Moreover, this also enables handling of water vapor in the exhaust gas for a dry ambient air and production of sulfur dioxide without referencing to another environment for fuels with sulfur content.

If the chemical mixing exergy from exhaust gases mixing with ambient air is omitted in both calculation of the exhaust gases and the fuel, it would neither show up in the work potential of the fuel nor as an irreversibility in the exhaust gas. For an ideal gas the exergy, when the exhaust to ambient air chemical mixing exergy is omitted, is calculated by

$$\varepsilon = \underbrace{h - h_\infty - T_\infty (s_{\text{th.}} - s_{\text{th.,}\infty})}_{\text{thermomechanical}} + \underbrace{\frac{C^2}{2}}_{\text{kinetic}} \quad (2.57)$$

If the work potential from different gas compositions between the exhaust gases and the ambient air would be omitted, for which the possibility is discussed in the previous section, the fuel exergy term needs to be adjusted accordingly. This implies that the equilibrium composition should be seen as the composition after combustion, which alters the chemical fuel exergy formulation accordingly:

$$\begin{aligned} \varepsilon_{\text{fuel,chemical}} = & \sum_i (\beta_i - \lambda_i) \cdot (\Delta h_{f,i}^\circ - T_\infty \Delta s_{f,i}^\circ) \\ & + T_\infty \left(\left[\sum_i \beta_i R_i \ln \frac{\beta_i M_i}{\sum_j \beta_j M_j} \right] - \left[\sum_i \lambda_i R_i \ln x_{\text{post combustion},i} \right] \right) \quad (2.58) \end{aligned}$$

A similar alteration is also valid for the Jet A specific calculation in Eq. 2.53. Moreover, it shall be noted that complete combustion formulations in Eq. 2.55 & 2.56 are left unchanged for the assumption of neglecting the exhaust to ambient air chemical mixing exergy.

The neglect of this mixing chemical exergy alters fuel exergy on more variables than the temperature, pressure and composition of the fuel, and the ambient conditions. Therefore, this assumption becomes more problematic when innovations are studied against each other that leads to different post-combustion gas compositions. Moreover, such assumptions also reduce the comparability between different propulsion unit exergy assessments. Furthermore, the neglect can also be said to violate the fundamental principle to measure the theoretical work potential. Thus, when considering to neglect the chemical mixing exergy between exhaust gases and the ambient air it is important to state it clearly and assess whether it is applicable for the specific type of study.

2.4 Application of Exergy to Non-standard Propulsion Components

General propulsion unit components for commercial aircraft can be incorporated into the framework outlined above. However, for radical engine concepts, some alternations might be required. Therefore, both detailed analysis of heat exchanger and closed systems, e.g. a secondary Rankine cycle, are enabled below. An analysis that breaks up the components of the exhaust irreversibility is also featured to aid better understanding of the loss mechanism.

2.4.1 Exergy Analysis of Heat Exchangers

By using the heat transfer exergy flux term in the irreversibility equation, it is possible to split a heat exchanger into several control volumes, as illustrated in Fig. 2.4. The upper part of the schematic illustrates the temperature profile along an axis perpendicular to the wall. The figure also includes the hot side static bulk temperature, T_h , found on the left side and the cold side static bulk temperature, T_c , on the right side. Both

temperatures are illustrated by the dashed temperature profile. In contrast to the first law of thermodynamics analysis, the heat transfer flux for the exergy analysis decreases in magnitude as the temperature reduces in the direction of the heat transfer flux. A control volume enclosing both sides of the process (dash-dot line) only includes mass flow-related exergy fluxes over the system boundary. However, this representation does not allow for a detailed picture of the intercooler (heat exchanger) irreversibilities. It becomes a question of how to represent the heat exchange process using a control volume approximation. When considering a scenario where a hot side control volume rejects heat at T_h and the heat enters the cold side at T_c , the heat loses work potential between these states. Hence, an additional control volume is needed for the considered scenario to incorporate all irreversibilities in the heat exchange process. This will however still not allow for an analysis that separates the losses from the different sides of the heat exchanger.

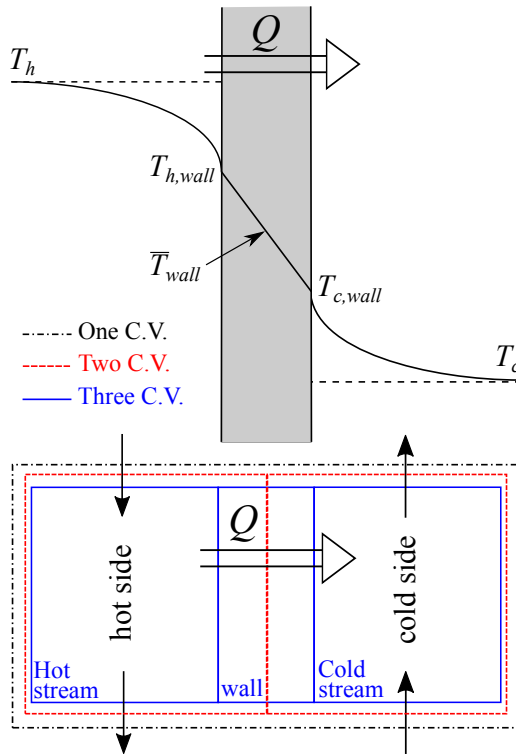


Figure 2.4: Heat exchanger control volume considerations. Above: the dashed lines represent the bulk temperatures for the hot and cold sides. The solid line represents the actual temperature profile and that the heat is losing quality over the boundary layer. Below: possible control volume considerations (using different colors) that either enclose the full heat exchange, treat fluid and wall separately or alternatively split the hot and cold side in the middle of the wall.

A more physical representation can be derived when taking into account that the fluid temperature at the wall surface will be affected by the heat transfer. Therefore, consideration of the wall temperature in the heat transfer exergy flux term of Eq. (2.2) yields the actual irreversibilities of each side. As the wall temperature is different between the two sides, a third and intermediate control volume is needed (blue line in Fig. 2.4). The intermediate control volume reflects the conduction through the wall. Heat exchangers are usually made out of metals, for which the thermal conductivity is high, leading to a small temperature drop through the wall. Thereby, it is assumed that an average wall temperature, \bar{T}_{wall} , can be used to separate the hot and cold side losses without any additional third control volume,

$$\sum_i \int_{\text{start}}^{\text{end}} \frac{\bar{T}_{\text{wall}} - T_\infty}{\bar{T}_{\text{wall}}} d\dot{Q}_i = \sum_i \dot{Q}_i \left(1 - T_\infty \frac{\ln [\bar{T}_{i,\text{wall, end}} / \bar{T}_{i,\text{wall, start}}]}{\bar{T}_{i,\text{wall, end}} - \bar{T}_{i,\text{wall, start}}} \right). \quad (2.59)$$

By imposing isobaric conditions between the start and end points of the heat exchange process, the irreversibility associated with the heat transfer itself can be estimated. This term can be subtracted from the total irreversibilities to obtain the lost work potential arising from the pressure loss.

2.4.2 Exergy Analysis in Closed systems

The exergy equations presented above originate from an open systems analysis. If addressing a closed system, e.g. a secondary Rankine cycle, then the equations need to be re-written. For a closed system, the working fluid is bound to stay in the cycle. For an aero-engine with a closed cycle incorporated the equilibrium velocity is thus equal to the flight velocity rather than to the zero absolute velocity. The thrust power must also be equal to zero as the mass is contained in the closed system. Put differently, there is no need to introduce the power thrust term, as the equilibrium velocity is equal to the flight velocity, into the energy equation, Eq. 2.16, which later forms the governing exergy equation for an open system detailed in Eq. 2.28 & 2.29.

Temperature and pressure are, however, limited by the ambient conditions. As the cycle is not adiabatic it can exchange heat until no temperature gradient exists, i.e. the limit is the ambient temperature. The internal equilibrium pressure of a rigid closed system would be a function of the working fluid thermodynamical behavior, the ambient temperature, the working fluid mass and the closed system volume. However, at this point there is still some theoretical work potential as the closed system could, in theory, expand until the internal pressure is in equilibrium with the ambient pressure. By combining the energy conservation equation, derived from the first law of thermodynamics, with the irreversibility derived from the second law of thermodynamics, in combination with the Gouy-Stodola relation, an additional irreversibility rate term is found applicable to closed

systems moving with the aircraft for a finite number of one-dimensional in- and outflows,

$$\dot{I}_{cs} = \left(\sum_i \dot{m}_i \epsilon_{cs,i} \right)_{in} - \left(\sum_i \dot{m}_i \epsilon_{cs,i} \right)_{out} - P_S + \sum_i \int \frac{T - T_\infty}{T} d\dot{Q}_i. \quad (2.60)$$

As the equilibrium conditions are different for the closed cycle the specific exergy term is also different. The kinetic specific energy compared to the equilibrium conditions is now calculated based on the relative velocity rather than the absolute velocity. Also, for a closed system, the equilibrium chemical composition is not different from the conditions present in the cycle. The chemical component of the specific exergy must thus be zero. Therefore, the entropy terms will only have a thermomechanical contribution. The specific mass exergy from Eq. 2.26 now becomes:

$$\underbrace{\epsilon_{cs}}_{\text{Work potential}} = \underbrace{h - h_\infty + \frac{V^2}{2}}_{\text{Total energy}} - \underbrace{T_\infty (s_{th} - s_{th,\infty})}_{\text{Inaccessible energy}} \quad (2.61)$$

The new specific exergy equation only relies on relative stagnation properties and is therefore easy to integrate into an engine performance code. Static entropy does not differ from stagnation entropy since stagnation is obtained when the fluid is brought to rest in an isentropic process. Still, the closed system irreversibility equation (Eq. 2.60) shows that the heat transfer exergy term depends on static properties. However, for lower velocities, so that T_0 is approximately equal to T , an analysis can be made that completely avoids assessing the static properties in the closed system moving with the aircraft,

$$\sum_i \int_{start}^{end} \frac{T - T_\infty}{T} d\dot{Q}_i = \sum_i \dot{Q}_i \left(1 - T_\infty \frac{\ln [T_{0,i,end}/T_{0,i,start}]}{T_{0,i,end} - T_{0,i,start}} \right). \quad (2.62)$$

2.4.3 Exergy Analysis of Exhaust Gases

The irreversibility of exhaust gases can be separated into different types of irreversibilities. This allows for a more detailed analysis and interrelating the different irreversibilities to the conventional performance measures. The control volume of the exhaust gases stretches between the nozzle outlet to the point where the exhaust gases are in complete equilibrium with its environment. The mass content exergy flows are therefore only different at the inlet face of the control volume. This analysis also has a thrust power term in the pressure difference to ambient conditions, i.e. the pressure thrust power in Eq. 2.34, previously detailed in the motivation leading up to the term. The pressure thrust power is a thermomechanical power term which leads to lowering of the thermomechanical losses. As the pressure thrust power term here is the pressure power doing work on the boundaries it takes away the mechanical part of the thermomechanical exergy. Thus, the thermomechanical irreversibility can be rewritten to thermal irreversibility, which better

describes the "source" of the loss. The irreversibility components, which together form the total exhaust irreversibility, become

$$\begin{aligned}
 \dot{I}_{\text{thermal}} &= \left(\sum_i \dot{m}_i \varepsilon_{\text{thermomechanic}} \right)_{\text{exhaust}} - P_{T_{\text{exhaust}} \rightarrow \infty}, \\
 \dot{I}_{\text{kinetic}} &= \left(\sum_i \dot{m}_i \varepsilon_{\text{kinetic}} \right)_{\text{exhaust}} \quad \text{and} \\
 \dot{I}_{\text{chemical}} &= \left(\sum_i \dot{m}_i \varepsilon_{\text{chemical}} \right)_{\text{exhaust}}.
 \end{aligned} \tag{2.63}$$

3 Exergy and Aircraft Performance

This chapter begins by relating the exergy methodology to conventional system performance variables. Installation effects of the propulsion subsystem are also assessed leading up on installed rational efficiency. Mission assessments are finally made building on the previously detailed exergy theory.

3.1 Relation between Exergy and Conventional Performance

To aid the understanding of the exergy methodology, the following section elaborates on the relation between conventional performance and exergy performance using conventional system performance variables. Starting with the relation between overall efficiency, that relates the added power to the thrust power, and the propulsive rational efficiency for a jet engine it can be noted that the expression only differs by the fuel enthalpy and the fuel exergy. The overall efficiency is:

$$\eta_{\text{overall}} = \frac{P_{\text{Tprop. unit}}}{\dot{m}_{\text{fuel}} h_{\text{fuel}}} \quad (3.1)$$

where the fuel enthalpy $h_{\text{fuel}} = \text{LHV} + [h - h_{\text{ss}}]_{\text{fuel-table}}$.

The propulsive rational efficiency for a jet engine, which does not include other power terms that might be seen as useful for the system, becomes:

$$\Psi_{\text{propulsive}} = \frac{P_{\text{Tprop. unit}}}{\dot{m}_{\text{fuel}} \varepsilon_{\text{fuel}}} \quad (3.2)$$

Relating these efficiencies to the specific fuel consumption, SFC, which equals the fuel consumption per thrust unit, i.e. $\frac{\dot{m}_{\text{fuel}}}{F_{\text{net}}}$, yields the following expression:

$$\text{SFC} = \frac{U}{\Psi_{\text{propulsive}} \varepsilon_{\text{fuel}}} = \frac{U}{\eta_{\text{overall}} h_{\text{fuel}}} \quad (3.3)$$

The overall efficiency can also be written as a product of the thermal efficiency, which relates the added power to the kinetic and pressure power, and the propulsive efficiency, which relates the kinetic and pressure power to the trust power, namely,

$$\eta_{\text{overall}} = \eta_{\text{thermal}} \eta_{\text{propulsive}}. \quad (3.4)$$

The thermal efficiency is written

$$\eta_{\text{thermal}} = \frac{\dot{E}_{\text{kinetic \& presure}}}{\dot{m}_{\text{fuel}} h_{\text{fuel}}}, \quad (3.5)$$

and the propulsive efficiency,

$$\eta_{\text{propulsive}} = \frac{P_{\text{Tprop. unit}}}{\dot{E}_{\text{kinetic \& pressure}}}. \quad (3.6)$$

The kinetic and pressure power is equal to generated power by the thermodynamic cycle. The generated power composes of two parts; the useful, i.e. thrust power (Eq. 2.35), and the wasted generated kinetic power. The wasted generated kinetic power is the exhaust kinetic irreversibility (Eq. 2.63) minus the kinetic power/exergy rate relative atmosphere at rest from the injected fuel, as the fuel already has kinetic power before being injected into the combustion chamber, which thus, shall not be considered as generated by the thermodynamic cycle. The formulation is

$$\dot{E}_{\text{kinetic \& pressure}} = P_{\text{Tprop. unit}} + \sum_i \dot{I}_{\text{kinetic},i} - \sum_i \dot{E}_{\text{x,fuel,kinetic},i}. \quad (3.7)$$

It is also possible to write the propulsive efficiency based on only the thrust power and wasted kinetic power, namely

$$\begin{aligned} \eta_{\text{propulsive}} &= \frac{P_{\text{Tprop. unit}}}{P_{\text{Tprop. unit}} + \sum_i \dot{I}_{\text{kinetic},i} - \sum_i \dot{E}_{\text{x,fuel,kinetic},i}} \quad \text{or} \\ &= 1 - \frac{\dot{I}_{\text{kinetic}} - \sum_i \dot{E}_{\text{x,fuel,kinetic},i}}{P_{\text{Tprop. unit}} + \sum_i \dot{I}_{\text{kinetic},i} - \sum_i \dot{E}_{\text{x,fuel,kinetic},i}}. \end{aligned} \quad (3.8)$$

For a jet engine, the fuel mass flow is significantly smaller than the overall mass flow, and therefore, the fuel kinetic power term can be neglected in the propulsive efficiency equation. This formulation becomes interesting within the scope of relating the exergy methodology to conventional performance numbers as the propulsive efficiency relates the thrust power to the exhaust kinetic irreversibility and vice versa.

3.2 Installation Effects on Exergy

The net thrust generated by the engine is propelling the aircraft. As long as the aircraft does not accelerate the forces that act on the aircraft must be in equilibrium with each other. This means that the net thrust is compensating for the drag of the aircraft. Utilizing the thrust required to compensate for any subsystem or component of the aircraft gives an opportunity to assess the impact a component or a subsystem has on the cycle. These forces multiplied with the flight velocity will correspond to the thrust power, or thrust work per unit time, that the propulsion unit is required to generate in order for the aircraft to stay on the path. From Eq. 2.35 it can be seen that the thrust power generated by the propulsion cycle equals the net thrust force multiplied by the flight velocity. When adding up the thrust power required to compensate for all the aircraft components this will in steady state match the thrust power generated by the propulsion cycle. It is worth remembering that the only work produced from an aircraft system perspective is the

change in altitude, all other power that originates from the fuel will be used to compensate for the direct drag, lift caused drag and other irreversibilities of the aircraft system.

To assess the impact of the drag and weight one must start by balancing the forces that act on the engine. A schematic of the acting forces and the axes for a generic aircraft is provided in Fig. 3.1. The angle between the aircraft axis and the aerodynamic axis is the angle of attack the aircraft has towards the air, α . The aerodynamic axis is parallel to the trajectory of the aircraft. The attitude, θ , is corresponding to the angle the aircraft has towards the horizontal plane. The climb gradient, γ , is instead the angle that the aircraft is moving in compared to the horizontal plane, which implies that $\gamma = \theta - \alpha$. The propulsion unit is mounted with an angle δ to the aircraft axis, and the axis made up by δ will be in line with the direction of the thrust. Moreover, if a thrust vectoring capability existed, this angle named δ would be allowed to change in flight. Lift is perpendicular, and drag is parallel to the aerodynamic axis of the aircraft. The weight force will act in the direction of the vertical axis.

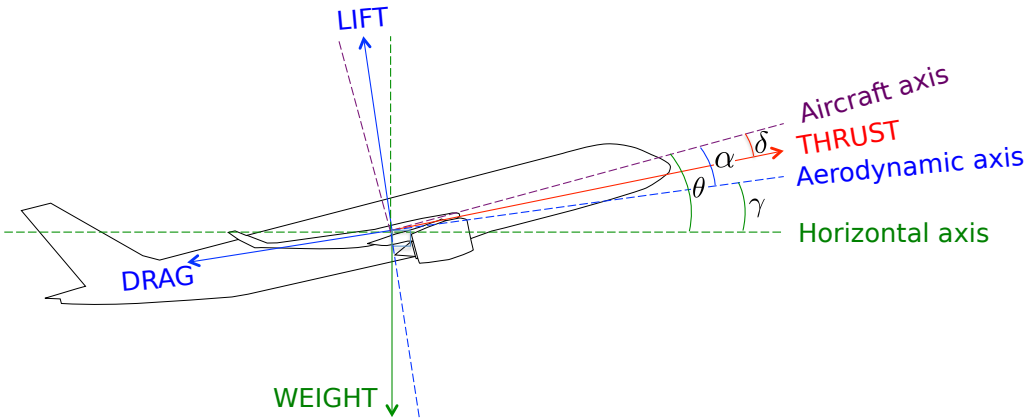


Figure 3.1: Main forces acting on an aircraft and its main directions.

At the inlet of the propulsion unit, air that is at rest with the atmosphere is sucked into the engine. By considering the velocity direction of the control volume face relative to the the propulsion unit (see Fig. 2.2), it can be noted that the momentum drag vector, \vec{F}_{md} , at the intake is parallel to the flight trajectory. The thrust vector, \vec{F}_g , on the other hand, is directed axially with the propulsion unit outlet. Therefore, the control volume face angle ϕ from Fig. 2.2 is zero between the momentum drag vector and the flight trajectory, whereas ϕ for the thrust vector is equal to $\alpha - \delta$. These vector thrust quantities have the following magnitudes:

$$F_g = \left(\sum_i \dot{m}_i V_i \right)_{\text{exhaust}} + \sum_i A_{\text{nozzle-exit},i} (p_{\text{exhaust},i} - p_\infty) \quad (3.9)$$

$$F_{\text{md}} = \left(\sum_i \dot{m}_i V_i \right)_{\text{intake}} \quad (3.10)$$

The force balances in the direction parallel to and the direction perpendicular to the flight trajectory become

$$\begin{aligned} ma_D &= -D + F_g \cos(\alpha - \delta) - F_{\text{md}} - mg \sin(\gamma) \text{ and} \\ ma_L &= L + F_g \sin(\alpha - \delta) - mg \cos(\gamma). \end{aligned} \quad (3.11)$$

The analysis is intended to yield a power balance, i.e. work per unit time. Work is assessed as the force applied in the trajectory direction multiplied by the object velocity and integrated over time. The drag equation is summing up the forces in the direction of the object trajectory. If a L/D number is assumed to be known the drag term can be altered accordingly

$$ma_D = -\frac{L}{L/D} + F_g \cos(\alpha - \delta) - F_{\text{md}} - mg \sin(\gamma). \quad (3.12)$$

Using the lift equation in Eq. 3.12 gives

$$\begin{aligned} ma_D &= -\frac{m(a_L + g \cos(\gamma)) - F_g \sin(\alpha - \delta)}{L/D} + F_g \cos(\alpha - \delta) - F_{\text{md}} - mg \sin(\gamma) \\ &= F_g \cos(\alpha - \delta) - F_{\text{md}} + \frac{F_g \sin(\alpha - \delta)}{L/D} - mg \sin(\gamma) - \frac{m(a_L + g \cos(\gamma))}{L/D}. \end{aligned} \quad (3.13)$$

Rearranging the equation gives the thrust terms on one side and the mass terms on the other. The force in the velocity direction times the velocity itself can be assessed using a scalar product of the respective vectors in the general work equation integrated over time. A scalar product of two vectors can be computed as the multiplication of the vector magnitudes and the cosine function of the angle between the vectors. With this in mind, it can be seen as ambiguous that there is both a cosine function as well as another term on the left-hand side. It should then be noted that these contributions actually originate from two different forces. The cosine term is the direct influence from the gross thrust in the direction of the flight trajectory. The other term corresponds to the thrust force perpendicular to the flight trajectory, in the direction of the lift, which alters the required lift that in turn affects the drag. This term shall however not be seen as drag directly caused by the lift. Drag originates from a combination of drag sources and lift over drag includes both the drag from the lift as well as drag present without considering the lift.

$$F_g \left(\cos(\alpha - \delta) + \frac{\sin(\alpha - \delta)}{L/D} \right) - F_{md} = m \left(a_D + \frac{a_L}{L/D} + g \sin(\gamma) + \frac{g \cos(\gamma)}{L/D} \right) \quad (3.14)$$

Multiplication of the flight velocity on both sides gives the equation on a power unit. The left-hand side can be split up in two terms. One of the terms equals the thrust power generated by the propulsion unit, and the other quantifies the loss due to misalignment between the thrust and the flight direction. This right-hand side can be divided into two parts: a dissipating and a non-dissipating and hence exergy accumulating part. The steady state contribution of the non-dissipative part is accumulated as the potential power in climb and can, later on, be harvested during descent. The acceleration terms will add to the momentum and are by definition non-dissipative.

$$\underbrace{U(F_g - F_{md})}_{\substack{\text{fully aligned} \\ \text{propulsion unit}}} - \underbrace{UF_g \left(1 - \left[\cos(\alpha - \delta) + \frac{\sin(\alpha - \delta)}{L/D} \right] \right)}_{\text{misalignment}} = mU \left(\underbrace{a_D + \frac{a_L}{L/D}}_{\text{acceleration}} + \underbrace{g \sin(\gamma)}_{\text{potential}} + \underbrace{\frac{g \cos(\gamma)}{L/D}}_{\text{dissipative}} \right) = \quad (3.15)$$

The terms on the left-hand side above can be exchanged into thrust power terms, it is

$$P_{T,ideal} = P_{T,prop. \text{ unit}} - P_{T,misalign.} \quad (3.16)$$

Multiple sources of drag exist in the context of an aircraft. Drag can be divided into three different groups; they are profile drag, induced drag and wave drag. Profile drag includes skin friction drag, form drag, and interference drag. The sources originate from the forces due to skin friction, the pressure distribution over the aircraft body and the mixing of streamlines over the body. Wave drag is the drag created by shock waves, and is therefore, only present in either transonic or supersonic flight. The induced drag originate from vortices that are created on the tip of the wing that in turn change the angle of attack which creates additional drag. These drag sources will partly originate from the lift while the other part is present independently from the current lift force. It is a common practice to separate the drag equation into one contribution that is independent of lift and another that is a function of lift. All the aforementioned contributing groups of the drag have a part that is due to lift. Induced drag is only due to lift, whereas the profile and wave drag have contributing parts that are either a function of, or independent of lift.

An arbitrary aircraft component or a subsystem could by itself add lift and drag in various ways. Such analysis might become complicated when one starts to consider where to put the boundary of each component as the aircraft consists of a large number of integrated

components. It also becomes a question of how the weight of one component should be matched to the corresponding drag force. Roth and Mavris included an aircraft loss breakdown over a mission profile, in terms of a technology assessing availability method named gas horsepower. The wave drag, skin friction and form drag over the fuselage, the tails and the external equipment stores of a Northrop F-5E fighter were considered [29, 30]. Their analysis also assessed the wings that in addition to the loss sources of the other components also include induced drag and lift. Different standards exist in aircraft design that allocate component weights into groups that correspond to a much more detailed breakdown of the weights than wings, fuselage, tails and external equipment stores. Such a standard could be used for an in-depth installed exergy analysis, but would, however, require an extensive effort put towards attributing the drag loss source to the right component. Roth also introduced the idea of distributing the corresponding fuel loss to the weight of each component [31]. This idea could be developed further in the frame of exergy analysis by charging the additional thrust power required to carry the weight of the fuel corresponding to the different component irreversibilities as part of the component losses themselves.

Paulus and Gaglioi extended the installed exergy analysis by assessing the exergy of lift in subsonic flight [32]. The exergy of lift relies on the minimum drag associated with the lift to stay at constant altitude for a component with an associated weight. The minimum drag corresponding to the weight that the wings are supposed to carry is not seen as an irreversibility of the wings but rather attributed to the different components weights. Such analysis requires information about the aircraft wing surface area and aspect ratio. It could be discussed which drag loss allocation scheme to carry a weight is the most appropriate. Whereas Paulus and Gaglioi allocate only the minimum drag lift to each weight one could also consider that a certain component with a given weight would if the weight was altered, affect the lift requirement more than just the minimum drag associated with the weight change. Such change also affects drag that is not dependent on the lift since a symmetric wing that is not generating lift still causes drag at a wing angle of attack at zero. Furthermore, a potential weight change also affects the drag associated with the non-ideal lift-caused drag. Note that an analysis that allocates all the losses associated with a component weight to the component also requires full knowledge about the total lift-caused drag. Which allocation to use becomes a matter of perspective, both allocation schemes will most likely yield different interesting insights of the system.

If one instead considers a components contribution to the overall losses independent on its geometrical shape, this allows an analysis dependent only on weight. The argument supporting such assumption would be that the components together constitutes the aircraft's outer geometrical shape, and it would be very hard to relate each components contribution to the outer geometrical shape. Using Eq. 3.15 for an independent component or subsystem implies an assessment of the impact based on the weight that needs to be compensated for by the propulsion unit. The impact of each component is then assumed to correspond to their weight averaged share of the total thrust requirement as the lift over drag number is taken as the aircraft metric. This allows for an analysis that requires less information about the aircraft as a whole, which can be useful when only analyzing a

component or subsystem. It could also be possible to combine this analysis with the assessment of the independent drag power if such information is known. This would, however, require the analysis to be altered slightly as the drag from the component itself is included in the total lift to drag ratio number.

3.2.1 Propulsion System Exergy Assessment

The full performance of the propulsion subsystem is not only the thrust generated from the propulsion unit. The propulsion subsystem has the main purpose of generating thrust towards the aircraft. The thrust required to compensate for the fact that the propulsion subsystem adds weight and causes additional drag for the aircraft is not beneficial for the aircraft system in terms of transporting wings, fuselage, fuel, passengers, and cargo. Hence, these irreversibilities should be included as irreversibilities of the propulsion unit in a system assessment. This yields an analysis that considers the full performance of the propulsion unit rather than the performance of the thermodynamic cycle itself.

If the drag directly associated with the propulsion system is possible to evaluate the force quantity, it yields can be used for computing the power drag associated with the propulsion subsystem. Here we consider a propulsion unit clearly separated from the wings and body of the aircraft. The drag power, as the drag force is in the negative direction of the flight trajectory, can be estimated accordingly:

$$P_{D,prop. syst.} = -UD \quad (3.17)$$

The balance of a single drag force and the thrust required to compensate for it yields the following expressions in Eq. 3.18 and Eq. 3.19. The first is including the misalignment of thrust with the flight trajectory while the second neglects misalignment and assumes that it is included in another thrust power term.

$$P_{T,prop. syst.-D incl. misalign.} = \frac{1}{\cos(\alpha - \delta)}UD \quad (3.18)$$

$$P_{T,prop. syst.-D excl. misalign.} = UD \quad (3.19)$$

The drag caused by a conventional ducted fan engine would mainly be made up by the nacelle drag. It is also possible to include drag from the pylon in the analysis even though it would have a smaller impact.

If the lift caused drag associated with the weight could be estimated it would be possible to use the thrust power drag equations detailed above. This would lead to an exact assessment of the thrust power required to compensate for the weight of the propulsion system. However, such analysis would require extensive information about the aircraft wings which in many cases is not known in a propulsion system performance assessment.

The weight caused drag associated with the propulsion system can also be seen as the weight-normalized share of the drag using Eq. 3.15. Using the direct engine drag in

combination with the weight-normalized drag from engine would be analogous to the installed specific fuel consumption formula, namely

$$\text{SFC}_{\text{installed}} = \frac{\dot{m}_{\text{fuel}}}{F_{\text{net}} - D_{\text{nacelle}} - D_{\text{from engine weight}}}, \quad (3.20)$$

where the drag caused by the engine weight is

$$D_{\text{from engine weight}} = \frac{m_{\text{engine}}g}{L/D_{\text{aircraft without nacelle}}}. \quad (3.21)$$

It shall be noted that the lift over drag number should ideally be altered in the weight thrust power equation to exclude the propulsion system drag in the denominator as the direct propulsions system drag is already compensated for in Eq. 3.18. However, the drag for the propulsion system is expected to be significantly lower than the total drag. In addition, the terms in Eq. 3.15 that include the lift over drag number have a rather small impact on the equation. With this in mind, the lift over drag number could be assumed as the true aircraft value.

The formulations for the thrust power to compensate for the propulsive system weight are detailed in Eq. 3.22 and Eq. 3.23. The first equation includes misalignment of thrust with the flight trajectory and the second disregards misalignment and assumes it to be included in another thrust power term.

$$P_{\text{T,prop. syst.-W incl. misalign.}} = \frac{Um_{\text{prop. syst.}} \left(a_D + \frac{a_L}{L/D} + g \sin(\gamma) + \frac{g \cos(\gamma)}{L/D} \right)}{1 - \frac{F_g}{F_g - F_{\text{md}}} \left(1 - \left[\cos(\alpha - \delta) + \frac{\sin(\alpha - \delta)}{L/D} \right] \right)} \quad (3.22)$$

$$P_{\text{T,prop. syst.-W excl. misalign.}} = Um_{\text{prop. syst.}} \left(a_D + \frac{a_L}{L/D} + g \sin(\gamma) + \frac{g \cos(\gamma)}{L/D} \right) \quad (3.23)$$

It should be noted that the sinus term in the misalignment factor could be omitted as it is at least two orders of magnitude smaller than the cosine term for a conventional aircraft.

The weight to compensate for a conventional aero engine would be the engine itself and the pylon holding the engine. It shall be noted that engine weight is not only a burden for the system since it also contributes to wing-load alleviation. This is, however, a secondary effect which is complex to assess. It could also be possible to include the fuel weight associated with the irreversibilities of the propulsion system.

The potential energy stored during the climb phase is not lost for the system. Instead, it can be harvested in descent to lower the thrust requirement to stay on the path. Due to this difference towards the other terms of the weight thrust power equation, it will be denoted

$$P_{T,\text{prop. syst.-D stored pot.}} = \begin{cases} Um_{\text{prop. syst.}}g \sin(\gamma) & \text{if } \gamma > 0 \\ 0 & \text{if } \gamma \leq 0 \end{cases} \quad (3.24)$$

When the aircraft is in descent the potential exergy term is turning negative, this implies that the exergy that was stored as potential energy during the climb phase is now harvested. The term becomes

$$P_{T,\text{prop. syst.-D harvested pot.}} = \begin{cases} 0 & \text{if } \gamma > 0 \\ Um_{\text{prop. syst.}}g \sin(-\gamma) & \text{if } \gamma \leq 0 \end{cases} \quad (3.25)$$

3.2.2 Installed Rational Efficiency

A new term, installed rational efficiency was proposed by Thulin et al. [7], to assess the full impact of the propulsion subsystem as a means to produce thrust for the aircraft. An equation to constitute the following pseudo equation was sought

$$\Psi_{\text{system,inst.}} = \frac{\text{Useful thrust power for the aircraft}}{\text{Consumed exergy}} \quad (3.26)$$

The useful power generated by the aero engine is the thrust it provides to the aircraft as well as the other useful power terms (Eq. 2.6), such as the cabin bleed and power that the propulsion system potentially supplies to the cabin. Compared to the rational efficiency in Eq. 2.5 the installed rational efficiency also takes the drag and the weight associated with the propulsion system into account.

It could be debated whether the misalignment between the propulsion system and the flight trajectory should be considered separately from the propulsion system or not. For a conventional engine, contrary to a unit with a thrust vectoring capability such as a tilted rotor concept, it can be argued that the misalignment should be included in the propulsion system performance. On the other hand, misalignment can also be included to accommodate the aforementioned concepts more appropriately. Both options are presented herein, the measure that does not include the full misalignment still includes the misalignment for installation effects of the propulsion system. The installed rational efficiency leaving the misalignment aside is

$$\Psi_{\text{system,inst. excl. misalign.}} = \frac{\begin{bmatrix} P_{T,\text{prop. unit}} \\ -P_{T,\text{prop. syst.-D incl. misalign.}} \\ -P_{T,\text{prop. syst.-W incl. misalign.}} \end{bmatrix} + P_{\text{other useful}}}{\begin{bmatrix} \dot{m}_{\text{fuel}}\varepsilon_{\text{fuel}} \\ -P_{T,\text{prop. syst.-D stored pot.}} \\ +P_{T,\text{prop. syst.-D harvested pot.}} \end{bmatrix}} \quad (3.27)$$

If one instead would include the misalignment into performance of the propulsion system it would lead to the following expression for the installed rational efficiency, it is

$$\Psi_{\text{system,inst. incl. misalign.}} = \frac{\left[\begin{array}{c} P_{T,\text{prop. unit}} \\ -P_{T,\text{prop. syst.-D excl. misalign.}} \\ -P_{T,\text{prop. syst.-W excl. misalign.}} \\ -P_{T,\text{misalign.}} \end{array} \right] + P_{\text{other useful}}}{\left[\begin{array}{c} \dot{m}_{\text{fuel}}\varepsilon_{\text{fuel}} \\ -P_{T,\text{prop. syst.-D stored pot.}} \\ +P_{T,\text{prop. syst.-D harvested pot.}} \end{array} \right]}. \quad (3.28)$$

This equations considers the control volume of the propulsion subsystem. It reflects upon the energy that is being stored as potential exergy as not consumed at that time instance but rather when it is being harvested and leaves the control volume.

3.2.3 Mission Assessment

The rational efficiency found in Eq. 2.5 or the proposed installed rational efficiency detailed in Eq. 3.27 and Eq. 3.28 can also be used for mission assessments of the performance of the propulsion unit or propulsion subsystem, respectively. All these equations yield the efficiency as a fraction of two quantities on a power unit basis at a specific time instance. If the performance is evaluated over a time frame, such as a full aircraft mission, the assessment has to be on a work unit basis, i.e. power unit integrated over time. The mission rational efficiency becomes:

$$\Psi_{\text{mission}} = \frac{\int_t (P_{T,\text{prop. unit}} + P_{\text{other useful}}) dt}{\int_t (\dot{m}_{\text{fuel}}\varepsilon_{\text{fuel}}) dt} \quad (3.29)$$

The installed mission rational efficiency formulations are detailed in Eq. 3.30 and Eq. 3.31. The first formulation regards the misalignment of the thrust and the flight trajectory as outside the performance of the propulsion subsystem while the second formulation includes it.

$$\Psi_{\text{mission - syst., inst excl. misalign.}} = \frac{\int_t \left(\left[\begin{array}{c} P_{T,\text{prop. unit}} \\ -P_{T,\text{prop. syst.-D incl. misalign.}} \\ -P_{T,\text{prop. syst.-W incl. misalign.}} \end{array} \right] + P_{\text{other useful}} \right) dt}{\int_t \left(\left[\begin{array}{c} \dot{m}_{\text{fuel}}\varepsilon_{\text{fuel}} \\ -P_{T,\text{prop. syst.-D stored pot.}} \\ +P_{T,\text{prop. syst.-D harvested pot.}} \end{array} \right] \right) dt} \quad (3.30)$$

$$\Psi_{\substack{\text{mission - syst,} \\ \text{inst incl. misalign.}}} = \frac{\int_t \left(\left[\begin{array}{c} P_{T,\text{prop. unit}} \\ -P_{T,\text{prop. syst.-D excl. misalign.}} \\ -P_{T,\text{prop. syst.-W excl. misalign.}} \\ -P_{T,\text{misalign.}} \end{array} \right] + P_{\text{other useful}} \right) dt}{\int_t \left(\left[\begin{array}{c} \dot{m}_{\text{fuel}} \varepsilon_{\text{fuel}} \\ -P_{T,\text{prop. syst.-D harvested pot.}} \\ +P_{T,\text{prop. syst.-D harvested pot.}} \end{array} \right] \right) dt} \quad (3.31)$$

Reference environment

Exergy is a property quantified as the work potential between the current state and an equilibrium state. For a propulsion unit the surroundings will be the ambient conditions and as previously described the ambient conditions stretches far enough that the gas flow in the aero engine will not change the ambient conditions. The ambient conditions will change drastically over an aircraft mission in terms of temperature and pressure. Rosen studied the impact of the choice of reference environment during a mission and concluded that having the reference environment constant, rather than changing with the mission, will lead to significant errors in the exergy analysis [33]. A reference environment other than the current ambient condition will lead to that the incoming air contains a magnitude of exergy different from zero. This incoming exergy cannot be used for the propulsion unit and will cause either a loss or a gain in the exhaust of the propulsion unit that has nothing to do with the true performance. A reference environment that varies in line with the mission points of the aircraft mission will lead to a true assessment of the propulsion system work and irreversibilities.

3.3 CFD-based Exergy Analysis for Aircraft-Integrated Propulsion Units

All the previous formulations have been derived to be used in system performance analysis. Exergy has also been applied in CFD analysis of combined aircraft and propulsion system simulations. Arntz and Merlen developed a theoretical framework for assessing aerospace applications through CFD studies [34]. This work targeted enabling precise analysis of a combined aircraft and propulsion system in a blended wing-body configurations with integrated propulsion units where the aerodynamics and the propulsion cannot be decoupled. The methodology was later on applied to the NASA Common Research Model [35], a geometric representation of a long-range wide-body twin-engine aircraft.

4 Variable Area Fan Nozzles

Turbofans featuring a greater bypass ratio, and consequently a larger fan diameter, in combination with a low fan pressure ratio (FPR) allows for achieving a desired thrust at a higher propulsive efficiency. The aerodynamic performance of the bypass section is in large dependent on the operation of the fan and the nozzle. The most efficient operation is a function of the combination of operating point fan efficiency and propulsive efficiency, and is constrained by the risk of surge and flutter. The need for fan surge margin at sea-level condition restricts the fan operation line for turbofans with low FPRs and fixed nozzles, which limits the performance over the whole flight envelope. Thus, a fixed nozzle turbofan design with a very low FPR implies a considerable matching problem between surge margin in take-off, efficiency in cruise and enough performance in top-of-climb. To understand more about why the operation becomes a more difficult matching problem for lower FPRs the reader is invited to study the outline presented by Thulin et al. [9].

A variable area fan nozzle enables a turbofan design that is less of a trade-off between efficiency and surge margin. The additional degree of freedom enables a larger surge margin during the more critical operating points, as the critical operation point surge margin now has less negative impact on the overall mission performance. Having more surge margin in critical points will limit stall flutter. Moreover, the risk of choke and unstalled supersonic flutter can be limited, on the other side of the operating range, by using area variability. The lower risk of flutter may in turn allow for lighter fan blades and thus penalize a larger fan less. In turn, this would enable design of UHBPR turbofans.

However, the potential improvements above come at the expense of adding additional weight to enable area variability. Smith [36] presented an assessment of performance and weight of a turbofan with a VAFN, which included some relative quantities of differences in weight and performance. That said, a methodology to assess weight of a variable area fan nozzle including absolute weight estimations had not previously not been made available in public literature before Thulin et al. presented a framework based on first principles to estimate weight from two down-selected variable area fan nozzle concepts in 2017 [9].

The two assessed concepts include the translating cowl concept and the multiple pivoting flaps concepts. A brief review follows below for the two concepts. For a more extensive review of these concepts as well as other reviewed concepts the reader is referred to study the work by Thulin et al. [9]

4.1 Translation of Rearmost Part of the Nacelle

The translating cowls concepts relies on translating the aft part of the cowl rearwards, by employing of actuators, to achieve a area variability. However, the cowl end's radial does not change. Rather, a different corresponding annular inner radius is obtained from the downward-sloping exhaust cone. This type of principle functionality is illustrated in Fig. 4.1 and has been proposed in different versions in patents US 5655360 A [37],

US5778659 A [38], and US8443586 B2 [39].

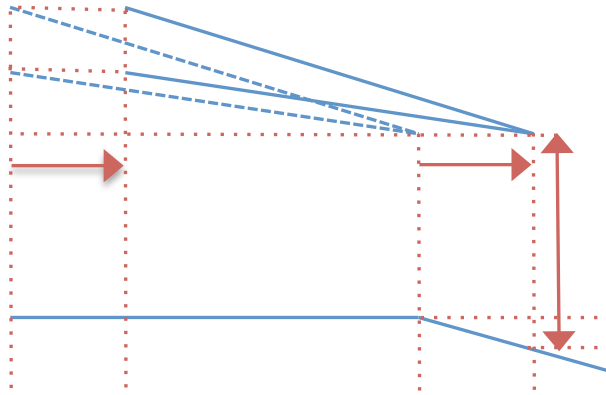


Figure 4.1: Working principle schematic using a translation of the rearmost part of the nacelle to enable fan nozzle area variability

4.2 Multiple Pivoting Flaps

The multiple pivoting flaps feature as the name entails multiple segmented flaps placed along the nozzle edge, similar to its more well-known military counterpart. The flaps rotate synchronously, around each individual attachment to the engine, by the use of one common sliding ring. The principle is illustrated in Fig. 4.2 and was proposed in patents US 7721551 B2 [40], US 7721549 B2 [41], and US 7637095 B2 [42].

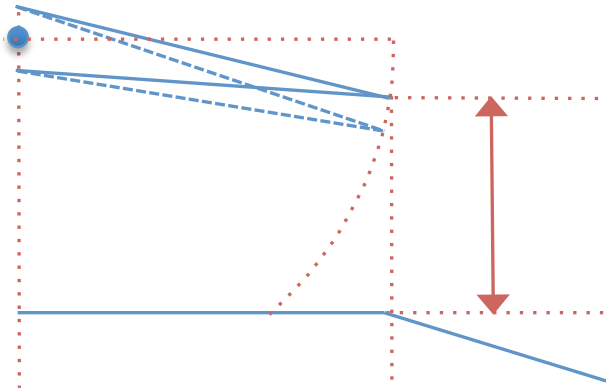


Figure 4.2: Working principle schematic using multiple pivoting flaps segmented around the nozzle edge to enable fan nozzle area variability

5 An Exergy Assessment of Modern Aircraft Engines and the Way Forward

This chapter assesses a modern turbofan. The reason for selecting this architecture is for its dominating market share in modern commercial aviation. The analysis is made from an exergy perspective to illustrate the major loss sources. The drivers of the major loss sources are detailed, and finally, an elaboration is made to elucidate the use of innovative technology that can address these losses, and thus, enable reduction of the carbon dioxide emissions from aviation.

5.1 State of the Art Aircraft Engines

A modern direct-drive two-spool turbofan corresponding to a technology maturity representative of the year 2020 was studied by the author in 2015 [7]. This analysis included the main points that constitute a mission, i.e. take-off, mid-climb, top-of-climb, begin-of-cruise, end-of-cruise, and descent. A mission assessment was made by summing the mission point contributions with the corresponding duration of the mission that in whole can be classified as a short-range mission for single-aisle aircraft. Based on this analysis a total mission exergy breakdown was made that included an installed subsystem perspective of what is useful for the aircraft, what needs to be compensated for in terms of added weight and drag from the engine and what is lost in the engine, see Fig.5.1. The engine losses were further detailed to assess the thermodynamic component contribution to the engine irreversibilities which is illustrated in Fig.5.2.

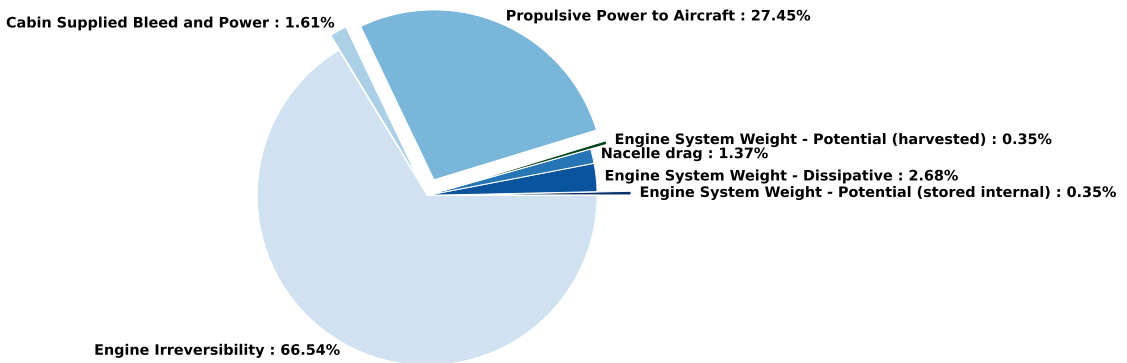


Figure 5.1: A short mission total exergy breakdown for a modern turbofan (Thulin et al. 2015 [7]).

The useful power generated by the propulsion system is the thrust it provides to the aircraft, the bleed and power it potentially supplies to the cabin, and finally, the potential energy that can be harvested in descent. The propulsive force generated by the turbofan amounted to 27.45% of the total work potential in the fuel. The cabin supplied bleed and power is about seventeen times smaller. Parts of the work it takes to lift the engine in the climb phase is not dissipative, rather it is stored as potential energy that can be harvested during descent. The part of the exergy that transforms from fuel exergy to potential exergy is not considered as consumed before it is harvested in descent where it adds to useful power, as means for gliding. The dissipative part of the installation effects corresponds to almost one eighth of the total propulsive force. Almost two-thirds of the total work potential is lost in engine irreversibility, this is also more than sixteen times larger than the dissipative installation effects.

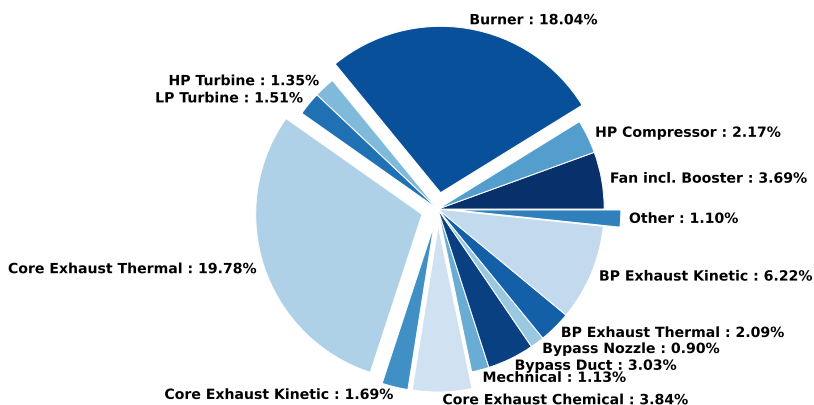


Figure 5.2: A short mission total engine irreversibility breakdown of a modern turbofan (Thulin et al. 2015 [7]). When the irreversibility percentages are summed up they correspond to the engine irreversibilities divided by the provided fuel exergy as illustrated in Fig.5.1.

The main loss sources in the turbofan can be found in the heat leaving the engine, the irreversibilities during combustion and the kinetic power that is not contributing to the propulsive force. These losses are further detailed below. It shall be noted that efficient turbomachinery and ducts are key for high system performance. In addition, since these parts are major weight drivers it is important that high efficiency is achieved at a low component weight. Turbomachinery that can achieve and resist high pressures and temperatures is also a key enabler for high cycle efficiency and to allow larger bypass ratios for higher propulsive efficiency. Moreover, well-designed ducts are also important for the performance of the other components. More information about the various loss sources is included in the enclosed article from the 2015 ISABE conference [7].

I shall be mentioned that the exergy methodology can also be used to evaluate future engines powered by other energy sources than common aviation jet fuel. Such energy sources could include bio-fuels, liquid natural gas, cryogenic hydrogen, stored electric

energy in batteries, solar power, etcetera. Nevertheless, the analysis herein has been stated to focus on the biggest irreversibility contributor components rather than the energy source since aviation is likely to be dependent on Jet A or similar bio-fuels for a considerable time going forward. Moreover, many components are generic to the type of energy source, and thereby, lowering of the respective losses would also be useful in case another energy source would be used.

5.1.1 Ejected Heat

A significant amount of work potential is lost for the system as hot gases leave the core exhaust without producing thrust. This is a result of that flow is energized in the engine cycle and then not brought to equilibrium with its surroundings. The thermal exhaust irreversibilities for the turbofan are illustrated in a temperature-accumulated normalized irreversibility chart provided in Fig. 5.3. The similarity of the hot side accumulated irreversibility up to, but not including, the exhaust, and a temperature-entropy diagram for Brayton cycle is striking. After all, the similarity is not surprising since the entropy production is directly proportional to irreversibility.

However, the irreversibilities for the exhaust gases are also illustrated, contrary to a normal temperature-entropy diagram. The core nozzle exhaust gases for the simulated engine is in excess of 380 Kelvin warmer (static properties) than the ambient temperature at cruise. Having higher thermal efficiency can help to limit the size of the core to reduce the ejected heat. The bypass flow also contributes to the ejected heat to a much less degree since the enthalpy increase in the bypass flow only takes place in the fan, where the specific enthalpy increase is very limited in comparison to in the core.

5.1.2 Combustion

Constant pressure combustion, as used in turbofans, is a process under which a significant amount of entropy is generated regardless of that the process is almost ideal. At a combustion efficiency of almost unity and a low-pressure loss coefficient, the combustion generates a substantial exergy loss. The burner irreversibility as a major loss source is rather an inherent effect of burning fuel as it generates a substantial amount of entropy.

It would be beneficial to combust at a steeper curve in a temperature-entropy (TS) diagram, i.e. during a path of increased pressure. To illustrate the difference to an ideal constant pressure combustion and an ideal pressure gaining combustion process, a combustion TS diagram is provided in Fig. 5.4. The figure includes the aforementioned Brayton cycle combustion processes, and an ideal constant volume combustion process, which also is known as a Humphrey cycle combustion process. It can be seen that the entropy production, and consequently the irreversibility, when keeping the combustion temperature constant reduces by about 1% when comparing the non-ideal Brayton combustion to its ideal counterpart, whereas it reduces by another 25% when the comparison is made to the ideal Humphrey combustion.

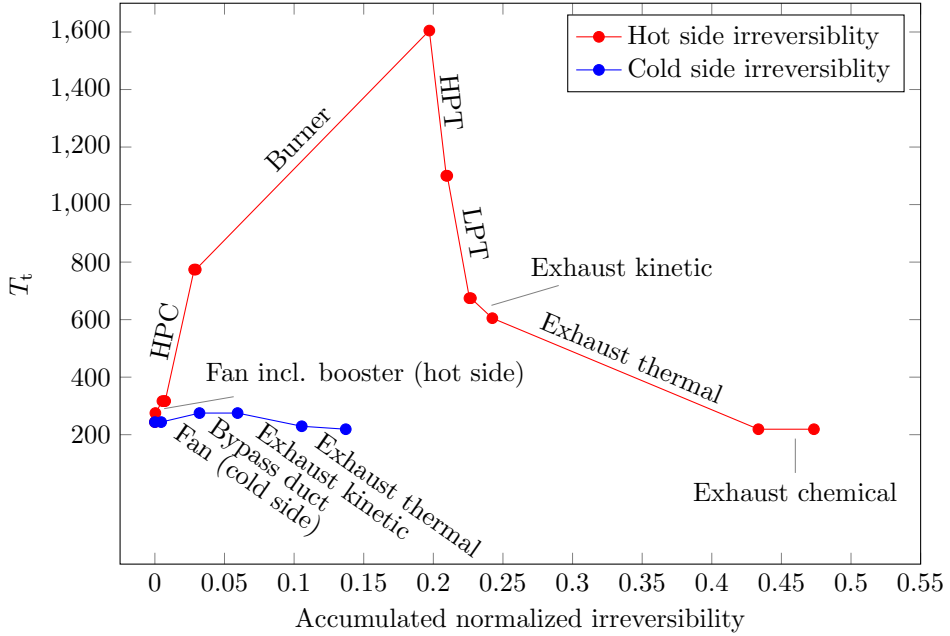


Figure 5.3: Temperature-accumulated irreversibility diagram provided for the hot and the cold side a turbfan engine during begin-of-cruise conditions (taken from Thulin et al. 2015 [7]). The accumulated irreversibility is normalized by the fuel exergy content. All the turbomachinery and duct component irreversibilities of the turbfan cycle are included. Components with the larger losses or larger total temperature differences pointed out.

To add to the combustion irreversibilities, the chemical exergy in the exhaust corresponding to a different gas composition compared to the ambient conditions is practically impossible to harvest. Hence, it can be seen as an inherent effect of burning fuel.

One dimension that is not directly considered within the exergy analysis is the formation of NO_x gases during the combustion process. NO_x also contributes to global warming, especially when emitted at high altitude, and therefore, it is a key aspect of a high-performance combustor to keep these emissions low.

5.1.3 Non-propulsive Kinetic Power

A propulsion unit produces kinetic and pressure power to create a thrust force that can power the aircraft forward. Part of the kinetic and pressure power in the nozzle is beneficial for the thrust to propel the aircraft, while another part is not. The thrust, based on the momentum equation, increases linearly with an increased nozzle velocity, while the kinetic energy increases quadratically. A lower thrust per mass flow unit, i.e. specific thrust, corresponding to the velocity difference between the nozzle velocity and flight velocity, in combination with higher total mass flow lowers these irreversibilities and

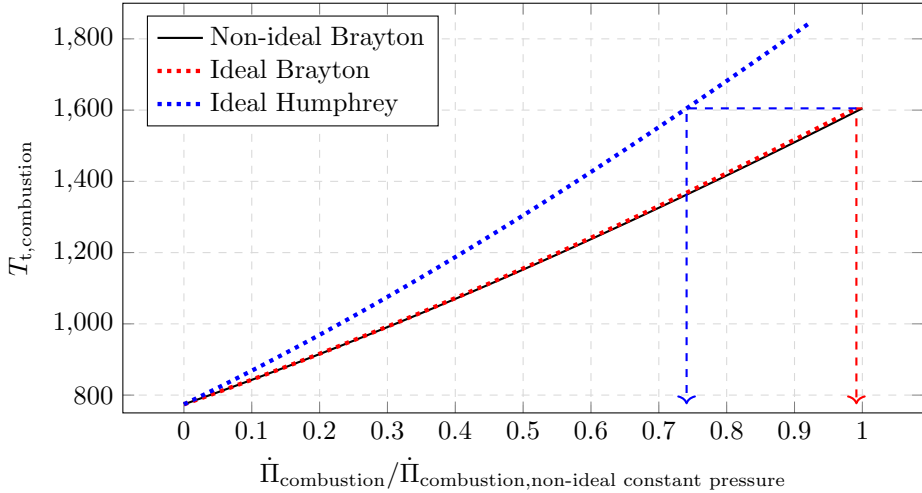


Figure 5.4: Comparison of normalized entropy production rate during the combustion of a non-ideal constant pressure combustion process (taken from Thulin et al. 2015 [7]), an ideal constant pressure combustion process, and an ideal constant volume combustion process. The two ideal processes are evaluated with similar fuel consumption as the non-ideal process, and all three are simulated during the begin-cruise operation point.

is simultaneously able to achieve the required total thrust. As a matter of fact, when the specific thrust goes towards zero these irreversibilities also goes towards zero. It was shown that the propulsive efficiency effectively relates the thrust and the kinetic exhaust irreversibility in Sec. 3.1 from being approximately equal to the thrust power divided by the thrust power and the kinetic exhaust irreversibility. To highlight how the propulsive efficiency increases by lower specific thrust its relation for an idealized jet engine is provided in Fig. 5.5. Moreover, the performance of a real turbofan is also provided during take-off, top-of-climb, and begin-of-cruise.

The quest towards higher propulsive efficiencies has been a key driver in commercial aviation when going from turbojets towards low bypass ratio turbofans and later to high bypass turbofans as higher bypass ratios allow for a large mass flow in combination with a low specific thrust. The bypass nozzle flow with its much larger mass flow is the dominating contributor to this loss source.

5.2 The Way Forward

Radical technologies that can be utilized to address the major loss sources previously detailed are now presented. Innovations attacking the lost thermal power, i.e. when the hot gases leave the core nozzle, are initially presented. Ways to tackle the major entropy

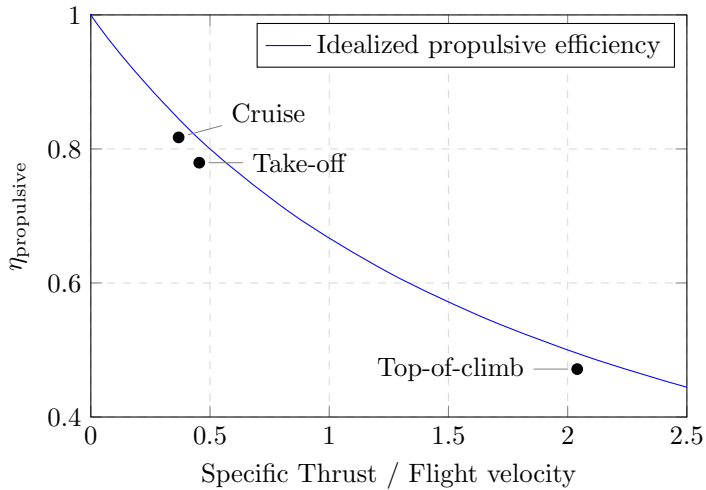


Figure 5.5: Propulsive efficiency is presented as a function of specific thrust over the flight velocity for an idealized jet engine, and during various operation points throughout a flight mission for a real turbofan (taken from Thulin et al. 2017 [9]). The idealized jet engine neglects the small mass flow contribution from fuel and assumes the nozzle to be non-choked.

generation during combustion are thereafter elaborated upon. Configurations aimed to achieve higher propulsive efficiencies are then finally featured.

5.2.1 Ejected Heat

Recuperation, i.e. preheating the compressed gases before combustion by heat exchanging from the hot exhaust gases, can recover some of the thermal energy leaving the engine without producing any thrust. By preheating the pre-combustion gases a lower fuel mass flow required to reach a given combustion temperature, and hence, it also allows for a reduction of the combustion entropy generation. The use of recuperation has been considered ranging back to the 1940s [43].

Intercooled cycles cool the gas between the intermediate and high-pressure compressor by heat exchanging to the bypass air. Zhao et al. studied an intercooled turbofan in 2016 using exergy [6] and indicated a 5.3% fuel reduction when utilizing intercooling and redesigning the studied geared turbofan. Intercooling allows for less work input per unit compression in the high-pressure compressor as it requires less energy to compress a cooler gas. Intercooling is also an enabler for higher pressure ratios as the corresponding high-pressure compressor exit temperature decreases to be within the limits of what the material can withstand. This advantage can be used to limit the core exhaust temperature, and hence, reduce the thermal energy in hot gases that are ejected from the nozzle.

A rather well-known innovative concept is utilizing the synergy that intercooling and recuperation can offer. The concept, the IRA engine, was presented by Boggia and Rüd 2004 [44]. By intercooling in the compression process, the temperature difference during recuperation increases, and thus, enables a larger heat transfer with lower losses per unit of heat transfer. Intercooling in combination with recuperating for turbofans has been considered since the 1970s but indicated no real benefit [45, 46, 47] at that time as the technology was not mature enough. A geared turbofan equipped with intercooling in combination with recuperation was assessed using exergy by Grönstedt et al. in 2014 [5] and yielded a 4.2% fuel burn reduction compared to the reference turbofan corresponding to a technology level to be representative of the year 2050.

Three other radical intercooling concepts were proposed by Petit et. al. [48]. These concepts proposed either to use the already available external nacelle surfaces as a heat sink of the intercooling process and thereby, to allow for a reduction of nacelle drag. Alternatively, to preheat fuel so that the heat later can be recuperated in the combustor. As a last the suggestion, to power a secondary Rankine cycle to create additional shaft power. The nacelle heat rejection and the secondary Rankine cycle intercooling concepts were later studied using the exergy framework by Thulin et al. 2017 [8] and yielded about similar performance levels as a geared intercooled reference engine with technology levels assumed to be available by the year 2025.

Other technologies that have been discussed to recover some of the thermal energy leaving the engine has been to employ a secondary Rankine cycle and to use inter-turbine reheating. A turbofan in combination with a secondary Rankine cycle for flight applications was analyzed by Perullo et al. in 2013 [49]. Stationary gas turbines using secondary Rankine cycles have been successful to reach unrivaled efficiency. Inter-turbine reheat by combustion between the first and a second turbine can allow for higher specific power density [50] for a maximum allowed turbine inlet temperature. This can help to lower the size of the core to reduce ejected heat as well as to support ultra-high bypass ratios.

5.2.2 Combustion

Piston engines were the predominant choice for powering aircraft until the mid-1950s. Already at this point, they featured pressures and temperatures unmatched by modern turbofans to yield specific fuel consumptions that match the most modern turbofan. Turbofans on the other hand offer a power to weight ratio that is outstanding, an extreme reliability as well as an inherently better ability to adopt to different ambient conditions as it does not suffer from a fixed stroke length. A composite engine cycle utilizing the possibility to achieve extremely high pressures and temperatures in a piston engine, as the peak conditions only apply temporary in the cyclic motion, in combination with the Brayton cycle was analyzed by Kaiser et al. in 2015 [51]. The idea was building upon a geared two-spool turbofan configuration. The concept outlined the idea to continue compressing the core mass flow coming from the intermediate pressure compressor by first utilizing a turbocharger succeeded by piston compressors. The compressed air is thereafter mixed

with fuel and ignited in piston engines under an initial isochoric combustion process which is continued by an isobaric combustion phase. The maximum peak pressure is corresponding to an overall pressure ratio at 300 in top-of-climb. After combustion process, the piston engine expands the air down to a pressure that corresponds to a temperature that can be handled after the Brayton combustion. Since a part of the combustion takes place during isochoric conditions, this will correspond to a steeper curve in the temperature-entropy (TS) which implies less entropy generation. The cycle will also increase in thermal efficiency as the pressure ratio increases which in turn enables a smaller core that can reduce ejected heat under the assumption that the hot gases leave the engine at the same temperature. Initial studies indicated a fuel burn reduction of 15.2% compared to the reference geared turbofan corresponding to technology maturity assumed to be available in the year 2025.

An alternative to achieve an intermediate combustion cycle is the relatively recent innovation provided by the nutating disc concept that was presented by Meitner et al. in 2006 [52]. The concept is achieving a constant volume for combustion by having a round plate enclosed in a combustion chamber, placed central to the axis of rotation and leaned from the perpendicular direction of the shaft to create a nutating motion (wobbling). The concept has the advantage of offering a structurally balanced constant volume combustion, as the mass center always coincides with the rotation axis, and to be relatively light. It has already been tested for unmanned aerial vehicles in hope to provide low vibrations, high efficiency, and compact installation. This concept could be used similarly to the piston engine topping of the Brayton cycle mentioned above.

A third alternative to achieve constant volume combustion that is not dependent on being combined with a conventional Brayton combustor to reach high temperatures is the pulse detonation combustion concept. In a conventional combustor, the combustion travels at ideally the subsonic flame temperature. If a detonation instead takes place, it will propagate supersonically through shock waves so that the gas does not have the time to expand. Rather, as illustrated by Wintenberger and Shepherd the flow compresses more than the Humphrey cycle during the initial shock wave [53]. Some of the pressure gains are later lost, but nevertheless, such cycle can theoretically allow for a higher pressure increase than the constant volume counterpart. The higher pressure generation also leads to the corresponding TS curve would be steeper in Fig. 5.4, which is also illustrated by Heiser and Pratt [54].

A concept that is relying on pulse detonation in combination with an intercooled and recuperated cycle and that promise to recover some of the dynamics generated by the detonation waves was assessed using the exergy by Grönstedt et al. in 2014 [5]. Stators at the outlet of the pulse detonation chambers turn the flow to allow for extraction of sonic wave kinetic energy in the following rotor stage. A fuel burn reduction was estimated to 18.8% in cruise compared to a reference turbofan corresponding to a technology level available in the year 2050. The irreversibilities comparing an intercooled and recuperated cycle to one with the difference of additional pulse detonation combustion went from 19.5% to 16.9% of the total irreversibilities for the respective configuration.

The pulse detonation concept relies some of the mass flow is used to push out the mass

flow where the detonation has taken place, i.e. the purge flow. Another concept that does not suffer of the requirement the detonation chambers to be purged after each detonation is the rotating detonating engine. This concept feature detonation waves constantly cycling around the annular shaped detonation chamber.

5.2.3 Non-propulsive Kinetic Power

It is possible to lower the irreversibilities related to kinetic energy leaving the engine without producing thrust by lowering the specific thrust and consequently the fan pressure ratio. To reach the same thrust requirement it is required to increase the mass flow. Open rotor and advanced geared ultra high bypass ratio turbofans allow for lower propulsive irreversibilities by enabling low specific thrust. Open rotor configurations rely on dual unducted counter-rotating rotors to replace the fan compared to a turbofan and can be designed to reach very high corresponding bypass ratios. A core of high power density, leading to a high overall pressure ratio, is key to enable powering the open rotor respectively the large fan blades.

To achieve higher BPR ratios for turbofans additional variability within the cycle might be required due to more changing operating conditions throughout the flight envelope. Two different types of variability that have been considered for this purpose are the variable pitch fan and the variable area fan nozzle. The variable pitch fan rotates the fan blades to adjust incidence and thus, optimizes the operation of the fan for specific conditions. The variable area fan nozzle adjusts the nozzle area to avoid fan surge in critical operating conditions. Furthermore, the variability can be used to optimize the operation throughout the whole flight envelope. This type of variability is further detailed within Sec. 4.

6 Summary of Papers

6.1 Paper A: A Mission Assessment of Aero Engine Losses

This article aimed to study the operation of a modern turbofan at the fundamental mission points throughout a commercial aircraft mission to establish how the losses of an aircraft engine are distributed today. The analysis also included installation effects of the propulsion unit, such as added system weight and nacelle drag that must be compensated for, to provide the *installed rational efficiency* measure that truly assesses the performance of the propulsion unit.

My contribution to the conference article was to carry out engine performance calculations, to implement an exergy accounting framework and to derive the installed rational efficiency term. The co-authors supervised the work and assisted in the analysis and writing.

It can be noted that the derivation of the installed rational efficiency term assumes the net thrust vector to be aligned with the engine outlet. However, as presented in this thesis, it should rather be the gross thrust, whereas the momentum drag is directed along the aerodynamic axis. Additionally, the formulation also neglects the sinus term in the misalignment factor. However, this does not change the results for the analysis as a conventional aircraft flies with the engine relatively aligned to the aerodynamic axis. The difference is estimated to be on a level of three orders of magnitude lower than the result of the initially proposed term at the most critical operating point. Furthermore, the weight irreversibility term itself is already small compared to the engine cycle irreversibilities. Hence, it becomes a small difference of an already small term.

6.2 Paper B: First and Second Law Analysis of Future Aircraft Engines

The article employs the exergy methodology for a cruise-point analysis to evaluate different future commercial engine concepts, including a turbofan reference corresponding to a technology level assumed to be available the year 2050, an intercooled and recuperated engine, a pulse detonation combustion engine and an open rotor engine [5].

My contribution to the journal article was to initially formulate the mechanics of the exergy methodology for implementation into a performance modeling software. This work was conducted within my joint master's thesis, that was carried out together with David Engerberg [55].

6.3 Paper C: First and Second Law Analysis of Intercooled Turbofan Engine

In this paper, geared intercooled turbofan cycles are studied using exergy and compared to a non-intercooled geared cycle. One of the intercooled cycles features an axial-to-radial high-pressure compressor, allowing for an ultra-high overall pressure-ratio. The design of this compressor is initially described. The exergy framework is later employed to further understand the benefits of intercooling.

My contribution to the journal article was to write the exergy theory section of the paper and to assist in the analysis of the exergy results.

6.4 Paper D: First and Second Law Analysis of Radical Intercooling Concepts

The aim of this paper is to extend the exergy framework for propulsion units to include a detailed analysis of heat exchangers, by allocating the irreversibilities to each side of the heat exchanger, and to provide an adequate formulation to handle closed systems, e.g. as a secondary Rankine cycle. Furthermore, the extended framework is used to study an intercooled reference engine and two recently proposed radical intercooling concepts. One of the radical intercooling cycle rejects the core heat in the outer nacelle surface, whereas the other uses the core heat to power a secondary Rankine cycle.

My contribution to this journal article was to derive the adequate formulations to handle detailed exergy studies of secondary cycles and heat exchangers. Moreover, to analyze the exergy results from the intercooled geared turbofan reference cycle, the nacelle intercooling cycle, and the secondary Rankine intercooling cycle. The co-authors assisted in the analysis and the writing. Carlos Xisto was the the main responsible for simulating the performance of the studied cycles, whereas I implemented the additional exergy formulations and assisted in the performance simulations.

6.5 Paper E: Variable Area Fan Nozzle Weight and Performance Modeling

The aim of this paper was to outline why a turbofan with a lower FPR experience more varying operating conditions and how a variable area fan nozzle capability can enable a less restricted operation. A review of different variable area fan is provided and two concepts are chosen in a down-selection. A weight assessment methodology based on first principles of the two down-selected variable area fan nozzle concepts is derived.

The implementation allows for a study to be made on the impact of the installation on performance.

My contribution to this scientific article was to outline the rationale for variable area fan nozzles for turbofans with low specific thrust. Moreover, I reviewed the different variable area fan nozzle concepts and derived the weight assessment framework of the down-selected concepts. Furthermore, I implemented the weight assessment of a variable area fan nozzle into an aircraft engine performance simulation software and to ran installed performance simulations. Finally, I also analyzed the results of the simulations. The co-authors supervised the work and assisted in the analysis and writing. Moreover, Tomas Gronstedt also set up the reference engine.

7 Summary of Contribution

An exergy framework has been developed to be used in state of the art engine performance codes to assess the component contribution to the overall system performance. The author was contributing to the first exergy studies on innovative engine concepts [5]. The investigated concepts included a turbofan reference corresponding to technology level assumed to be available in the year 2050, an intercooled and recuperated engine, a pulse detonation combustion engine and an open rotor engine. The author did also participate in a study on intercooling in turbofan aero engines to enable better understanding of the benefits of the concept [6].

The developed exergy framework was also applied to the first mission study of a modern turbofan that corresponds to a typical airline operation [7]. The major irreversibilities are shown to be the thermal energy leaving the turbofan in the core exhaust flow, the vast entropy production in constant pressure combustion, and the non-propulsive kinetic energy. All these losses are further detailed within the thesis, and possible ways of limiting them are elaborated upon.

By lowering the specific thrust, it is possible to reduce the non-propulsive kinetic irreversibility. Turbofans that are operating at lower fan pressure ratios experience more varying operating conditions throughout the flight envelope. Thus, an imposed additional variability to the cycle might be required to assure acceptable performance and at the same time reasonable safety margins towards critical operation. Therefore, the author studied the installation effect of two different variable area fan nozzles concepts and presented the first publically available method of assessing weight associated with such a system [9].

The exergy framework was further developed to accommodate analysis of aircraft engines featuring heat exchangers and secondary systems. This enabled detailed analysis of two radical intercooling concepts [8], where one used the nacelle surfaces for heat rejection and the other powered a secondary cycle.

The analysis by Thulin also presented the *installed rational efficiency* concept, a true measure of the propulsion system performance, by compensating for the weight and drag associated with the engine to assess the useful power to the aircraft [7]. The installation effects were also studied throughout the envelope of the mission to, finally, yield a mission total installed rational efficiency.

Using the developed framework to assess any propulsion system is beneficial for improved understanding of the component losses in the system. In conjunction with conventional performance analysis methods, this can then help exploring new innovative propulsion unit concepts in search for lower fuel consumption and thus lower emissions. To conclude, exergy analysis is not a new paradigm for propulsion unit system analysis, rather a beneficial complement that makes the analysis of complex propulsion unit systems much more straightforward.

Bibliography

- [1] J. M. Clarke and J. H. Horlock, "Availability and propulsion," *J Mechanical Engineering Science*, vol. 17, p. 223, 1975.
- [2] R. B. Evans, *A proof that essergy is the only consistent measure of potential work*. PhD thesis, Dartmouth College, 1969.
- [3] H. M. Brilliant, "Second law analysis of present and future turbine engines," in *31st Joint Propulsion Conference, San Diego, U.S.*, 1995. AIAA 95-3030.
- [4] B. Roth, R. McDonald, and D. Mavris, "A method for thermodynamic work potential analysis of aircraft engines," in *38th Joint Propulsion Conference, Indianapolis, U.S.*, 2000. AIAA 2002-3768.
- [5] T. Grönstedt, M. Irannezhad, L. Xu, O. Thulin, and A. Lundbladh, "First and second law analysis of future aircraft engines," *J Eng Gas Turb Power*, vol. 136, no. 3, 2014.
- [6] X. Zhao, O. Thulin, and T. Grönstedt, "First and second law analysis of intercooled turbofan engine," *J Eng Gas Turb Power*, vol. 138, no. 2, 2015.
- [7] O. Thulin, T. Grönstedt, and J.-M. Rogero, "A mission assessment of aero engine losses," in *22nd International Symposium of Air Breathing Engines, Phoenix, U.S. 2015, ISABE-2015-20121*, 2015.
- [8] O. Thulin, O. Petit, C. Xisto, X. Zhao, and T. Grönstedt, "First and second law analysis of radical intercooling concepts," *J Eng Gas Turb Power*, 11 2017.
- [9] O. Thulin, A. Lundbladh, and T. Grönstedt, "Variable area fan nozzle weight and performance modeling," *To be submitted to scientific journal*, 2017.
- [10] T. J. Kotas, *The Exergy Method of Thermal Plant Analysis*. Butterworths, 1985.
- [11] O. Reynolds, "Papers on mechanical and physical subjects," in *The Sub-Mechanics of the Universe*, vol. 3, Cambridge University Press, 1903.
- [12] R. Clausius, "Ueber eine veränderte Form des zweiten Hauptsatzes der mechanischen Wärmetheorie," *Annalen der Physik*, vol. 169, pp. 481–506, 1854.
- [13] S. Carnot, *Réflexions sur la puissance motrice du feu : et sur les machines propres à développer cette puissance*. Paris: Bachelier, 1824.
- [14] Y. Çengel and M. Boles, *Thermodynamics: an engineering approach*. McGraw-Hill series in mechanical engineering, McGraw-Hill Higher Education, 2006.
- [15] R. Clausius, "Über verschiedene für die Anwendung bequeme Formen der Hauptgleichungen der mechanische Wärmetheorie," *Annalen der Physik*, vol. 125, pp. 353–400, 1865.

- [16] S. Wright, M. Rosen, D. Scott, and J. Haddow, "The exergy flux of radiative heat transfer with an arbitrary spectrum," *Exergy, An International Journal*, vol. 2, no. 2, pp. 69 – 77, 2002.
- [17] R. Petela, "Exergy of heat radiation," *Journal of Heat Transfer*, vol. 86, pp. 187–192, 05 1964.
- [18] R. Petela, *Engineering thermodynamics of thermal radiation for solar power utilization*. New York: McGraw Hill, 2010.
- [19] A. Bejan, *Advanced Engineering Thermodynamics*. New York: John Wiley & Sons, second ed., 1997.
- [20] S. D. C., *Introduction to Thermodynamics*. London: Academic Press, 1964.
- [21] S. M. Jeter, "Maximum conversion efficiency for the utilization of direct solar radiation," *Solar Energy*, vol. 26, no. 3, pp. 231 – 236, 1981.
- [22] J. Szargut, D. R. Morris, and F. R. Steward, *Exergy analysis of thermal, chemical, and metallurgical processes*. New York: Hemisphere, 1988.
- [23] J. Szargut, "Chemical exergies of the elements," *Applied Energy*, vol. 32, no. 4, pp. 269 – 286, 1989.
- [24] I. Dincer and M. A. Rosen, *Exergy, Energy, Environment and Sustainable Development*. Elsevier, 2007.
- [25] B. J. McBride and S. Gordon, *Computer Program for Calculation of Complex Equilibrium Compositions and Applications*, 1994. NASA RP-1311.
- [26] Y. RAO, *Chemical Engineering Thermodynamics*. Orient BlackSwan, 1997.
- [27] ISO, "Standard atmosphere," standard, International Organization for Standardization, Geneva, CH, 1975.
- [28] Chevron U.S.A. Inc., *Aviation Fuels - Technical Review*, 2007. Available at https://www.cgabusinessdesk.com/document/aviation_tech_review.pdf.
- [29] B. Roth and D. Mavris, "A generalized model for vehicle thermodynamic loss management and technology concept evaluation," in *2000 World Aviation Conference*, American Institute of Aeronautics and Astronautics, 2000.
- [30] B. Roth, "Aerodynamic drag loss chargeability and its implications in the vehicle design process," in *1st AIAA, Aircraft, Technology Integration, and Operations Forum*, American Institute of Aeronautics and Astronautics, 2001.
- [31] B. Roth and D. Mavris, "Technology evaluation via loss management models formulated in terms of vehicle weight," in *59th International Conference on Mass Properties Engineering*, 2000. SAWE-2000-3001.

- [32] D. M. J. Paulus and R. A. Gaggioli, "The exergy of lift and aircraft exergy flow diagrams," *International Journal of Thermodynamics*, vol. 6, pp. 149–156, 2003.
- [33] M. A. Rosen, "Exergy losses for aerospace engines: effect of reference environment on assessment accuracy," *Exergy, an International Journal*, vol. 6, 2009.
- [34] A. Arntz, O. Atinault, and A. Merlen, "Exergy-based formulation for aircraft aeropropulsive performance assessment: Theoretical development," *AIAA Journal*, vol. 53, no. 6, pp. 1627–1639, 2014.
- [35] A. Arntz and D. Hue, "Exergy-based performance assessment of the nasa common research model," *AIAA Journal*, vol. 54, no. 1, pp. 88–100, 2015.
- [36] C. J. Smith, "Affordable nacelle technologies for future turbofans," *J Eng Gas Turb Power*, vol. 118, pp. 236–239, 04 1996.
- [37] L. Butler, "Thrust reverser with variable nozzle." 1997-08-12. US patent 5655360 A.
- [38] P. Duesler, C. Loffredo, H. T. P. J., and C. Jones, "Variable area fan exhaust nozzle having mechanically separate sleeve and thrust reverser actuation systems." 1998-07-14. US patent 5778659 A.
- [39] C. Loffredo and C. Szyszko, "Variable geometry exhaust nozzle for a turbine engine." 1998-11-10. US patent 5833140 A.
- [40] R. Hanson, "Fan variable area nozzle for a gas turbine engine fan nacelle." 2010-05-25. US patent 7721551 B2.
- [41] K. Baran, "Fan variable area nozzle for a gas turbine engine fan nacelle with cam drive ring actuation system." 2010-05-25. US patent 7721549 B2.
- [42] M. Winter and R. Hanson, "Thrust vectorable fan variable area nozzle for a gas turbine engine fan nacelle." 2009-12-29. US patent 7637095 B2.
- [43] "Notes on the bristol theseus heat-exchanger propeller turbine," *Aircraft Engineering and Aerospace Technology*, vol. 18, no. 11, pp. 366–371, 1946.
- [44] K. R. Stefano Boggia, "Intercooled and recuperated aero engine," in *41st AIAA/ASME/SAE/ASEE Joint Propulsion Conference & Exhibit*, 2004. AIAA 2005-4192.
- [45] J. D. Eisenberg, *A preliminary study of the use of intercooling and reheat in conjunction with regeneration for aircraft turbine engines*, 1977.
- [46] J. Kentfield, "Regenerative turbofans: a comparison with non regenerative units," *Journal of Aircraft*, vol. March, pp. 174–182, 1975.
- [47] D. Gray and J. Witherspoon, "Fuel conservation propulsion concepts for future air transports," *SAE paper number 760535*, 1975.

- [48] O. Petit, C. Xisto, X. Zhao, and T. Grönstedt, “An outlook for radical aero engine intercooler concepts,” in *Proceedings of ASME Turbo Expo 2016: Turbine Technical Conference and Exposition, Seoul, South Korea*, 2016. GT2016-57920.
- [49] C. Perullo, D. N. Mavris, and E. Fonseca, “An integrated assessment of an organic rankine cycle concept for use in onboard aircraft power generation,” in *Proceedings of ASME Turbo Expo 2013: Turbine Technical Conference and Exposition, San Antonio, U.S.*, 2013. GT2013-95734.
- [50] N. Yannakoulis, “Introducing inter-turbine reheat in a high-bypass civil turbofan engine,” Master’s thesis, Cranfield University, 2004.
- [51] S. Kaiser, S. Donnerhack, A. Lundbladh, and A. Seitz, “A composite cycle engine concept with hecto-pressure ratio,” in *51st AIAA/SAE/ASME Joint Propulsion Conference*, American Institute of Aeronautics and Astronautics, 2015.
- [52] G. Smith, P. Meitner, J. Jerovsek, and M. Boruta, “Meyer nutating disc engine: A new concept in internal combustion engine technology,” in *43rd AIAA/ASME/SAE/ASME Joint Propulsion Conference & Exhibit*, American Institute of Aeronautics and Astronautics, 2007.
- [53] E. Wintenberger and J. E. Shepherd, “Thermodynamic cycle analysis for propagating detonations,” *Journal of Propulsion and Power*, vol. 22, no. 3, pp. 694–698, 2006.
- [54] W. H. Heiser and D. T. Pratt, “Thermodynamic cycle analysis of pulse detonation engines,” *Journal of Propulsion and Power*, vol. 18, no. 1, pp. 68–76, 2002.
- [55] D. Engerberg and O. Thulin, “Aero engine exergy analysis,” Master’s thesis, Chalmers University of Technology, 2012.